Linnæus University

Master's Thesis in Structural Engineering

Optimized utilization of raw materials for production of Cross Laminated Timber

Quality of laminations and its effects on mechanical properties of multi-layer panels

Authors: Beatrice Larsson, Gustaf Lindstam
Surpervisor, LNU: Anders Olsson
Examinar, LNU: Björn Johannesson

Course Code: 4BY35E

Semester: Spring 2019, 15 credits

Linnaeus University, Faculty of Technology
Department of Building Technology

Abstract

Cross laminated timber (CLT) is a product increasingly demanded by the market. This has led to an interest among producers to further optimize the use of raw material. The aim of this investigation is therefore to analyze how the material properties in softwood lamellas, when used in different layers of a CLT plate, affect the stiffness and strength for CLT floor elements. This is done by analysis of CLT constructions with different dimensions, constructions and quality of lamellas. For the bending stiffness of CLT plates, the most important lamination property is the longitudinal modulus of elasticity. However, the stiffness to rolling shear of the lamellas has also large influence on the combined bending and shear stiffness of a CLT plate.

The properties for the lamellas that has being used in this investigation are valid for Norway spruce (*Picea Abies .L*). For investigation and analysis of the lamellas and the CLT floors has Finite Element simulations by the software Abaqus (2017) along with hand calculations been used. A total of three different simulations were performed to accomplish the objectives set in this work.

Notations

$\boldsymbol{\epsilon}$	Column matrix containing six strain components
ϵ_{LL}, ϵ_{RR}, ϵ_{TT}	Elastic normal strains in the orthotropic directions L, R, T.
γ_{LT}, γ_{LR}, γ_{RT}	Elastic shear strains in the orthotropic directions L-T, L-R, R-T.
$\boldsymbol{\sigma}$	Column matrix containing six stress components
σ_{LL}, σ_{RR}, σ_{TT}	Normal stresses in the orthotropic directions L, R, T.
τ_{LT}, τ_{LR}, τ_{RT}	Shear stresses in the orthotropic directions L-T, L-R, R-T.
E_L, E_R, E_T	Modulus of elasticity in the principal directions
G_{LR}, G_{RT}, G_{LT}	Shear modulus in the principal directions
$G_{XY,c,i}$	Rolling shear for a characteristic value.
ν_{LR}, ν_{LT}, ν_{RL}, ν_{RT}, ν_{TL}, ν_{TR}	Values for the Poisson's ratio in the principal directions
C	Compliance matrix
D	Stiffness matrix
k_{sys}	Lamination effect
I_{ef}	Effective moment of inertia
$I_{x,net}$	Net moment of inertia
$W_{x,net}$	Net flexural resistance
$EI_{eq.1}, EI_{eq.2}$	Equivalent bending stiffness
$E_{eq.1}, E_{eq.2}$	Equivalent modulus of elasticity
γ_i	Gamma value for layer *i*
F_{max}	Maximum force

Denominations for forces and moments

$f_{,k}$	Characteristic bending stiffness
$f_{t.0.k}$	Characteristic tension stiffness parallel to the fibers
$f_{t.90.k}$	Characteristic tension stiffness perpendicular to the fibers
$f_{c.0.k}$	Characteristic compression stiffness parallel to the fibers
$f_{c.90.k}$	Characteristic compression stiffness perpendicular to the fibers
$f_{v.090.xlay.k}$	Longitudinal shear in x-direction
$f_{v.090.ylay.k}$	Longitudinal shear in x-direction
$f_{v.9090.xlay.k}$	Rolling shear in x-direction
$f_{v.9090.ylay.k}$	Rolling shear in y-direction
f_d	Design bending strength

Acknowledgement

The collaboration with Södra Skogsägarnas has been great and we want to thank our supervisor at Södra Henrik Johansson for his support and engagement in the project. We wish Södra good luck with their new CLT production plant and that our work will contribute to efficient utilization of materials in production.

We also want to thank our supervisor Anders Olsson at Linnaeus University for all support and help in the project. Without Anders expertise and contribution with data from previous studies this research would not have been possible.

Table of Contents

1. Introduction

1.1 Background

Wood is one of the most important materials and one of very few renewable materials that are suitable for constructions. When working with wood products it is important to have knowledge of factors that affect the material and its properties. All properties of wood are linked to the cell structure and the composition of the stem such as moisture related deformation, decay resistance, strength properties etc. (Holmberg and Sandberg, 1997). As a product from the nature the possibility to influence the properties of a growing tree is limited. Genetic heritage, growth conditions and silvicultural measures is parameters affecting the timber properties of Norway spruce (*Picea Abies. L*) (Oscarsson, 2014).

Cross-laminated timber (CLT) is an Engineered Wood Product (EWP) used in building constructions as plates, panels or shells in floor, walls and roofs. CLT consists of an odd number of layers of lamellas, i.e. boards of wood, where each layer is oriented in perpendicular direction to the adjacent layers. Finger joints are used to produce lamellas long enough for production of large panels. Due to cross lamination, CLT elements are stiff and strong to tension, compression and shear in all in-plane directions and to out-of-plane bending (Gustafsson, 2017).

Construction with CLT is relatively new and was introduced in Austria and Germany in the early 1990's. The interest and demand for building with CLT has since then increased, especially since the early 2000's. The increased demand can be seen partly as result of the environmental awareness that has developed in the society during the last decades (Karacabeyli and Douglas, 2013). CLT is a material that has an eco-friendly cycle and can be expected to have a long lifecycle, just as solid wood, when it is protected from moisture. Therefore, CLT as a constructional material can compete with other materials used in construction, i.e. steel and concrete. At the same bearing capacity as a concrete element, a CLT element has less weight and is easier to handle and transport (Gustafsson, 2017).

In 2013 Austria, Germany and Switzerland were the largest producers of CLT with up to 90 % of the total production in the world (Stauder, 2013). The annual production of CLT in the world has increased from about 100 000 m^3 in 2005 to 700 000 m^3 in 2015 (Brandner et al. 2016). There are some estimates that the annual production in only Europe will reach 1.2 million m^3 in 2020 (Timber Online, 2019) and a future continued accelerated worldwide production of CLT can be expected in the years to come. The expected increased demand of CLT is a driving factor in the ongoing development of a harmonized standard for CLT products (Brandner et al., 2016).

The continuous development for CLT in the world is also discussed by Oscarsson and Blixt (2016) in a pre-study, demanded by industry, to investigate prerequisites for production of CLT in southern Sweden. The only producer in Sweden today (2019) is Martinsons with production located in Bygdsiljum in northern Sweden, with an annual production of 25 000 m^3 CLT products (Martinsons, 2019). However, this is about to change since several forest industries are developing CLT production plants. Södra Skogsägarna, Setra and Stora Enso are three companies in Sweden that plan to open manufacturing lines of CLT in 2019 – 2020 (Edholm, 2019).

With an increasing number of producers of CLT the importance for each producer to utilize their raw material efficiently to become more competitive on the market. An ideal scenario for a CLT producer is to obtain desired bearing capacity, utilizing the potential of high-quality timber and, at the same time, make use of as much low-quality timber as possible in the elements. This leads to an interest in evaluating different parameters i.e. quality and thickness of the layers of a CLT element. Properties of layers depend, in turn, on properties of the included lamellas.

1.2 Aim and objectives

The aim of this project was to evaluate how bending stiffness in CLT elements, to be used as plates in floors, are influenced by the quality of raw lamellas. By applying different values for material properties and different dimensions of the lamellas, calculation will give indication of how to obtain CLT panels with optimized structural properties. To achieve the aim, specific objectives are set to:

- Analyze the structure of wood and identify wood quality factors that may affect stiffness and bearing capacity of CLT elements.
- Evaluate how rolling shear in lamellas are influenced by the location of the pith.
- Establish models to calculate and present how stiffness in CLT elements changes when changing the longitudinal stiffness or the rolling shear of the lamellas used in the element.

1.3 Limitations

To make this research adapted to CLT production in Sweden and useful for the company Södra Skogsägarna and other producers in Sweden, this research focuses on Norway spruce (*Picea Abies L.*) as raw material in the CLT products. No other specie were considered. A limitation has also been set to only evaluate dimensions for lamellas and cross section which, according to Södra Skogsägarna, may be relevant for production of plates to be used as floors. Therefore, stiffness related to out-of plane bending and shear were the primary investigated parameter.

Only a limited statistical evaluation of differing material properties was considered in this research though only mean modulus of elasticity values from C-classed boards from Sweden, Norway and Finland were investigated.
Also, this research only investigated Norway spruce were characteristic strength and stiffness properties were considered.

No laboratorial tests were performed. The presented results are based on finite element analysis and hand calculations. To limit the area for analysis the research also has been limited to simulation of four-point bending tests of two CLT plates and evaluation of the influence of rolling shear by simulation of a three-point bending test of a CLT plate.

2. Theory

In relation to Sweden's total land area the country has large forest resources where 47 % of the standing forest volume consists of the softwood specie Norway spruce (*Picea abies L.*). The second most common specie is also a softwood specie, Scots pine (*Pinus silvestris L.*) which constitutes for 37 % of the volume. The remaining part is hardwood species such as birch, oak, ash etc. (Gross and Hansson, 1991). The softwood species comes from the botanical group gymnosperms and have a cross-section where the annual rings appear clearly (Casselbrant et al., 2004).

Heterogeneous and orthotropic are two words that are commonly used to describe wood as a material. Heterogeneous means that the material properties can vary greatly within a tree and between different trees, whilst orthotropic means that the material properties are different depending on direction in the material (Nylinder and Fryk, 2011). The heterogeneous properties are affected by the surrounding environment during its growth which means that geographic location where the lumber originates from is of great significance. Material variation comprises variations of important properties such as density, modulus of elasticity, shrinkage parameters and strength (Ormarsson, 1999).

2.1 Softwood growth and clear wood properties

On a microscopic scale the term clear wood is commonly used to describe wood as a material. On this analysis level orthotropic properties can be prescribed to the material by a matrix describing material properties in different directions. Three orthogonal axes can be defined for the material creating an LRT-coordinate system which are presented in *Figure 1.* The longitudinal direction (L) is parallel to the grain, the radial direction (R) is perpendicular to the growth rings and the tangential direction (T) is perpendicular to the longitudinal and radial directions (Majano-Majano et al., 2011).

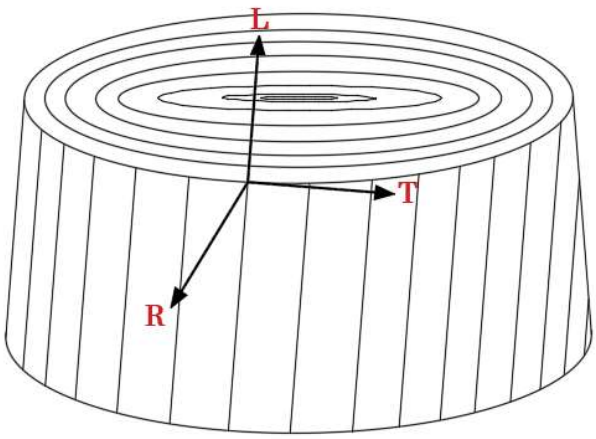

Figure 1: The principal directions for LRT-coordinates at a local point in the trunk of a tree.

Norway spruce has, compared to other species, small shrinking/swelling. The shrinking occurs first after the moisture content falls below the fiber saturation point, which is 30 %. From that point the percentage shrinkage for the three principal directions for drying Norway spruce to a 12 % moisture content are presented in *Table 1* (Holmberg and Sandberg, 1997).

Table 1: Shrinkage from the fiber saturation point to 12 % moisture content for Norway spruce with a density between 380-400 kg/m3 (Holmberg and Sandberg, 1997).

Shrinkage	**Percent [%]**
Longitudinal	0.2 – 0.3
Radial	3.6 – 4.2
Tangential	7.8 – 8-8

2.1.1 Cell structure

Softwood is composed by two cell types, tracheid and parenchyma cells. 95 % of a tree consists of tracheid cells which are the largest contributor to strength and stiffness properties. Parenchyma cells have very small influence on strength and stiffness properties and can thus be neglected with respect to mechanical properties (Persson, 2000). The tracheids are not precisely oriented along the longitudinal direction of the stem but with an angle to it, giving a so-called fiber angle (Ormarsson, 1999).

A tracheid cell can be divided into three parts, cell wall, cell lumen and middle lamella where the cell wall is the structural part of the cell. Lumen is as the cavity where most of the fluid transport occurs during growth. The middle lamella is the bond that connects cells to each other. Due to this fact is the cell wall of great significance in the matter of mechanical properties (Dinwoodie, 2000).

The cell wall is composed by small thread-like units called microfibrils creating a primary and secondary wall where the secondary wall consists of three layers. The primary wall is very thin with randomly orientated microfibrils. The layers of the secondary wall can be denoted as S_1, S_2 and S_3. S_1 and S_3 are the outer- and inner layers of the primary wall. The microfibrils in the S_1 layer are oriented with a 50º-70º angle and a 60º-90º angle for the S_3 layer. The dominating layer is though the S_2 layer which constitutes 70-80 % of the total cell wall thickness. The microfibrils in this layer can have an angle be in the range between 5º-45º which strongly effect the cell properties for stiffness and shrinkage (Ormarsson 1999).

2.1.2 Trunk structure

Due to the circular growth of the tree the material properties of wood are depending on the direction of the material. The circular growth rings are easy to identify by the naked eye in a cross-section of a stem. The production of a new growth ring is the result of cell production which takes place in the cambium just inside the bark of the stem. The growth season of a tree can be divided into spring and summer. During the spring, the so-called early wood is formed. This material contains cells with big lumen and thin walls, well suited for water transport. During summer, growth speed of the tree decreases and tracheids with thicker cell walls, so-called latewood, which add strength and stiffness to the tree. The difference in cell wall thickness gives earlywood a lower density than latewood (Persson, 2000).

Wood is divided into juvenile and mature wood. From the pith and outward, the first 15-20 annual rings consist of juvenile wood which has shorter tracheids with a higher microfibril angles and thinner cell walls. Lower bearing capacity and higher shrinkage in longitudinal direction compared to the mature wood is a result of the juvenile woods structure. Sapwood and heartwood are two other terms that describe the structure of the stem. The sapwood is the outer part of a stem, which contains of living cells that are responsible for the liquid transport in the stem. However, the cells in the inner rings eventually dies and the so-called mature wood is created. For spruce and pine the origination of mature wood starts after 10 – 30 years. Mature wood is less susceptible for shrinking and swelling since no liquid transportation occurs in the dead cells (Nylinder and Fryk, 2011).

Two other parameters that effects the material orientation are, first, the fact that the trunk of a tree is shaped like a cone rather than like a cylinder. This means that the tracheids, within the longitudinal-radial plane of the material, has an angel to the pith of the log called the conical angle. The second parameter is called the spiral grain effect and occurs in the longitudinal-tangential plane of the material and is the result of a spiral growth pattern of the tracheid in the growth layers. An angle between the longitudinal orientation of the tracheids and the pith appears as a result of the spiral growth which can cause twists on dried sawn

timber. The spiral grain angle is at its largest close to the pith of the tree and decreases with increasing distance to the pith (Säll, 2002).

2.1.3 Stiffness properties of Norway spruce clear wood

As pointed out earlier, the material properties in a tree trunk can vary considerably from pith to bark. The modulus of elasticity is depending on the microfibril angle in the S_2-layer which makes the modulus of elasticity low close to the pith and increasing when approaching the bark as a result of the juvenile woods high microfibril angle (Persson, 2000). The lumber that is closer to the bark of an old tree can possess an elastic modulus twice as high compared with the elastic modulus for lumber closer to the pith (Ormarsson, 1999). The strength and stiffness are much higher in the longitudinal direction compared with the radial and tangential direction due to the tracheid cells orientation. Smallest is the stiffness in the tangential direction where it is about 2/3 of the stiffness in radial direction (Persson, 2000).

Load rate, duration of loading together with environmental factors such as humidity and temperature affect the mechanical behavior of wood. Below the limit of proportionality wood behaves as a linear elastic orthotropic material which makes it possible to apply a cylindrical coordinate system for the LRT-coordinate system of a small wood piece. By the assumption of linear elasticity Hooke's generalized law can then be applied for the orthotropic material as

$$\boldsymbol{\epsilon} = \mathbf{C}\boldsymbol{\sigma} \tag{2.1}$$

where $\boldsymbol{\epsilon}$ is the elastic strain vector, **C** the compliance matrix and $\boldsymbol{\sigma}$ the stress vector. The expression can also be written in matrix from as

$$\begin{bmatrix} \epsilon_{LL} \\ \epsilon_{RR} \\ \epsilon_{TT} \\ \gamma_{LR} \\ \gamma_{LT} \\ \gamma_{RT} \end{bmatrix} = \begin{bmatrix} \frac{1}{E_L} & -\frac{\nu_{RL}}{E_R} & -\frac{\nu_{TL}}{E_T} & 0 & 0 & 0 \\ -\frac{\nu_{LR}}{E_L} & \frac{1}{E_R} & -\frac{\nu_{Tr}}{E_T} & 0 & 0 & 0 \\ -\frac{\nu_{LT}}{E_L} & -\frac{\nu_{RT}}{E_L} & \frac{1}{E_T} & 0 & 0 & 0 \\ 0 & 0 & 0 & \frac{1}{G_{LR}} & 0 & 0 \\ 0 & 0 & 0 & 0 & \frac{1}{G_{LT}} & 0 \\ 0 & 0 & 0 & 0 & 0 & \frac{1}{G_{RT}} \end{bmatrix} \begin{bmatrix} \sigma_{LL} \\ \sigma_{RR} \\ \sigma_{TT} \\ \tau_{LR} \\ \tau_{LT} \\ \tau_{RT} \end{bmatrix} \tag{2.2}$$

where E_L, E_R, E_T represents the modulus of elasticity and G_{LR}, G_{LT}, G_{RT} are the shear modulus in the different principal shear planes. ν_{LR}, ν_{LT} and ν_{RT} are values for the Poisson's ratios which are constants of strains that can be used for calculation of stresses in different directions.

The inverse of the **C** matrix can be expressed by

$$\mathbf{D} = \mathbf{C}^{-1} \tag{2.3}$$

which makes it possible to express the stress vector as

$$\boldsymbol{\sigma} = \mathbf{D}\boldsymbol{\epsilon} \tag{2.4}$$

For details, see Persson (2000).

2.1.4 Rolling shear in clear wood

Rolling shear is defined as shear stress acting in the plane of a laminated cross section perpendicular to the grain which leads to the emergence of shear strains. Rolling shear appears in a wood materials RT-plane, which is the direction in which the stiffness is weakest to shear. Because of the low rolling shear stiffness in timber, substantial deformation caused by shear can occur (Fellmoser and Blaß, 2004).

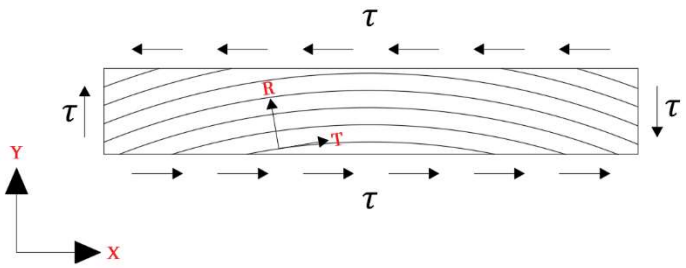

Figure 2: Stresses in a lamella causing rolling shear in RT-direction.

Figure 2 shows the RT-plane dependency on the orientation of the annual rings. In a research performed by Aicher and Dill-Langer (2000), the rolling shear modulus G_{XY}, i.e. the shear modulus was investigated with respect to the axes X and Y, and their correlation with the orientation of growth rings. This research was analyzed by finite element calculations. The result of that study showed a changing value for rolling shear stiffness in the XY-coordinate system between 50 N/mm^2 to 200 N/mm^2 depending on the orientation of the annual rings in the cross section.

The proportionality constant for the rolling shear module in the XY-coordinate system can be denoted as the relationship between the applied shear stress (τ) and the shear strain (γ). By knowledge of the force (F) acting in X-direction and distributed over a surface area (A), perpendicular to the XY-plane, the shear stress can be obtained by

$$\tau = \frac{F}{A} \tag{2.5}$$

The shear strain, γ_{XY}, which is the changes of angle of two, from the outset horizontal and vertical lines, respectively, of the cross section, depend on the applied force and can be calculated as

$$\gamma_{XY} = \arctan\left(\frac{\Delta x}{\Delta y}\right) \tag{2.6}$$

where Δx and Δy are the change in the x and y direction according to *Figure 3*.

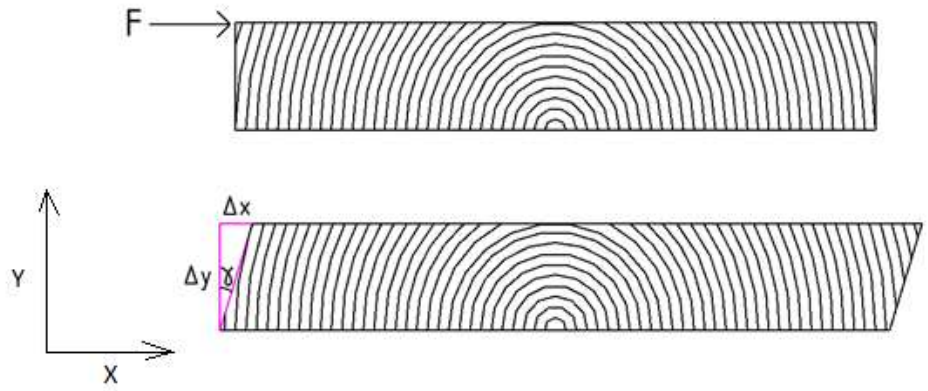

*Figure 3: Illustration of shear deformation in a lamella where the shear strain is depending on Δ*x *and Δ*y.

With knowledge of the values for shear stress and strain the rolling shear modulus, on the level of a lamination, can be calculated as

$$G_{XY} = \frac{\tau}{\gamma_{XY}} \tag{2.7}$$

2.2 Grading of sawn timber

Norway spruce sawn timber is commonly used in construction and buildings (Holmberg and Sandberg, 1997). In sawn timber the mechanical priorities vary due to sawing pattern and the appearance of knots. To reduce the scatter of the mechanical properties, sawn timber is graded into strength classes. In Europe sawn timber is graded into C-classes which declare five percent fractile and mean values of the mechanical properties of the classes, see the European standard EN 338:2016 (Stapel and van de Kuilen, 2013). In *Table 2* characteristic values for material properties for some common C-classes presented according to the standard EN 338:2016 (Gustafsson, 2017).

Table 2: Material properties for construction timber for some strength classes (EN 338:2016).

Properties	**C14**	**C16**	**C24**	**C35**
Strength values [MPa]				
Bending parallel to the fibers f_k	14	16	24	35
Tension parallel to the fibers $f_{t,0,k}$	7.2	8.5	14.5	22.5
Tension perpendicular to the fibers $f_{t,90,k}$	0.4	0.4	0.4	0.4
Compression parallel to the fibers $f_{c,0,k}$	16	17	21	25
Compression perpendicular to the fibers $f_{c,90,k}$	2.0	2.2	2.5	2.7
Shear $f_{v,k}$	3	3.2	4.0	4.0
Stiffness values [MPa]				
Mean value for modulus of elasticity parallel to the fibers $E_{m,0,mean}$	7 000	9 000	11 000	13 000
5-percentage fractile for modulus of elasticity parallel to the fibers $E_{m,0,05}$	4 700	5 400	7 400	8 700
Mean value for modulus of elasticity perpendicular to the fibers $E_{m,90,mean}$	230	270	370	430
Mean value for shear modulus G_{mean}	440	500	690	810
Density [kg/m^3]				
5-percentage fractile of density ρ_k	290	310	350	390
Mean value for density ρ_{mean}	350	370	420	470

When grading boards or lamellas to a C-class, it is required that 95% of that particular batch acquires strength and density properties in regard to the mentioned standard EN 338:2016. However, requirements regarding MOE the requirements apply to the mean value for MOE. Consequently, there is a variation in material properties between individual lamellas since quite different properties than the characteristic properties of the class to which they are assigned. Olsson and Oscarsson (2017) investigated how utilization of structural timber could be improved by suggesting a method to strength grade lamellas more accurately. This study evaluated 900 pieces of Norway spruce from Sweden, Norway and Finland to retrieve as reliable results as possible (Olsson and Oscarsson, 2017).

2.2.1 Influence of knots

Knots in sawn timber have a considerable effect on the mechanical properties of wood lamellas, though they are often the determining factor for strength. A knot has a higher density than clear wood, deviation fiber direction and moisture content compared to the surrounding wood which causes a disturbance in the material. The disturbance leads to stresses in direction perpendicular to the longitudinal direction of the material which reduces the stiffness and strength (Nylinder and Fryk, 2011).

2.2.2 Grading machines

Dynamic excitation of timber boards is used in grading machines to sort sawn timber into strength classes depending on a dynamic modulus of elasticity. This type of machine is equipped with an impact mechanism that strikes the end cross section of the board. The hit from the impact mechanism makes the board vibrate and generates soundwaves which are detected by microphones or laser vibrometers. When analyzed, the lowest resonance frequency is used to estimate the axial modulus of elasticity of the board, which in turn is used to predict the board's strength and stiffness parameters. Precigrader strength grading machine is an example of this type of machine. A precigrader measures not only resonance frequency but also dimensions and mass of the wood piece (Dynalyse, 2019).

Computer Tomography (CT) X-ray scanning is another technology that is used for strength grading. The outer surface of a log could sufficiently be investigated and presented with help from a 3D scanner. However, with CT scanning it is possible to reconstruct the internal features of a log, where internal features such as knots and cracks are analyzed and considered. It is due to the positioning of the knots and cracks that the CT scanner retrieves estimated values strength and stiffness. The log is also often subjected to rotation, from which the CT scanner can get more adequate information to evaluate. This is done to optimize timber yield and determine more precise strength grading (Rais et al., 2017).

Another technology/type of machine that can be used for grading is a surface scanner which can be used to grade sawn timber into strength classes. This method is deemed to be a relatively reliable approach though it uses a set of dot lasers along with multi-sensor equipped cameras that can collect data regarding fiber orientation on all surfaces of the lamellas. The wood scanner obtains data regarding fiber orientation by using the tracheid effect, which means that fibers in softwood are better to absorb light in the direction of the fibers rather than across (Matthews and Beech 1976) (Soest et al. 1993). The intensity of the light distribution that is detected is then summoned around the laser dots which later acquires the shape of an ellipse. These ellipses are oriented in direction of the softwood fibers, which provides a useful method for evaluating variations in grain angles on wood surfaces. This method is also useful when detecting knots, since wood fibers in knots are directed almost perpendicularly to the longitudinal direction of the lamella which creates light spots that are close to circular. Thickness, length and depth of the lamellas are also determined by the scanner, which later are used in order to define the indicating properties of the lamellas (WoodEye, 2015).

Over the years many authors have showed that more accurate predictions of bending strength can be made if knowledge regarding local MOE is taken into consideration, where the local MOE is measured over a few centimeters (Oscarsson et al. 2014). Wood scanners used in the industry today mainly for visual inspection, could also be utilized for accurate assessment of local MOE (Olsson and Oscarsson, 2017).

2.3 Cross laminated timber products

CLT elements are a versatile product that can be used for a variety of things, from small to large scale. However, the main area of use is for floors and walls which makes them suitable for both smaller, simpler buildings and multi-story building with higher demands of fire protection and sound isolation. The large cross-sectional area, which CLT elements often possesses, contributes to a high stiffness as well as high load-bearing capacity, which makes them suitable to stabilize various structures. The weight of CLT elements are relatively low compared to other construction material which benefits transport and assembly of buildings (Gustafsson, 2017).

The cross-lamination procedure that is used to obtain CLT elements creates a structure with profitable stiffness properties in more than one direction of the material. The movement of moisture within the material also becomes small due to the cross lamination and a symmetric cross section. Today in 2019 there is, however, still no approved and standardized strength classes for CLT elements (Gustafsson, 2017). Moreover, the strength classes that are used for laminations are developed for different purposes than for CLT laminations. These strength classes used for laminations are also based on the five percent fractile of strength.

A CLT element usually consists of 3, 5 or 7 layers of lamellas that are glued perpendicular to the adjacent lamellas, where it is common to use lamellas with a thickness between 20 and 45 mm. The layers usually have the same size but is also quite common that the inner layers are of different sizes. Common maximum dimensions of a produced CLT element is 3 x 16 meters but elements of larger size exist, as well as elements consisting of more than 7 layers. Odd number of layers are always used in the construction to obtain CLT element to reduce moisture related deformations (Gustafsson, 2017).

Since CLT elements are constructed from raw lamellas it is necessary to emphasize the difference between material properties in single lamellas and the properties in larger CLT elements as a whole. As mentioned before raw lamellas can have different properties such as density, stiffness and strength, depending on e.g. growth area, placement in the log and the presence of knots. In CLT elements the variation of properties between laminations are smoothed out in the cross laminated panel. The phenomenon is called the system effect and result in less variation in properties within and between elements (Gustafsson, 2017).

The density in CLT elements is also representative for the density in raw lamellas. However, CLT elements obtains a density that is relatively close to the mean value of the density of the laminations. This makes the variations in density of CLT elements relatively small compared to the variations in density between raw lamellas (Brander and Bauer, 2016).

Just as density, the moisture content in CLT elements are also representative for the moisture content that occurs in raw lamellas. As with other Engineered Wood Products (EWP), CLT is also influenced by shrinkage and swelling due to moisture content variations (prEN 16351:2018).

2.3.1 CLT as floors – plates subjected to bending and shear

Vibrations and springiness of floors affects the total experience of quality in buildings. How severe vibrations that occur in turn depends on the stiffness of the floor construction. When CLT elements are used as plates in a floor structure the stiffness to bending and shear depend on the construction and layer design of the CLT elements.
Stable and comfortable flooring can therefore be achieved by dimensioning and designing sufficiently stiff CLT elements. Flat flooring elements, cassette-hole elements and composite elements are three different construction types of CLT elements. The most commonly used in floors are flat flooring elements, which is the type considered in this research. In flat flooring elements the loads are transferred by the element as a whole and distributed further to the underlying construction. Flat flooring elements must be designed to have high cross-sectional bending stiffness. They also have small moisture induced strains due to the cross lamination (Gustafsson, 2017).

The lamellas in the CLT element's main bearing direction are decisive for the structural element's strength and stiffness properties. However, lamellas oriented in direction perpendicular to the main bearing direction are subjected to so called rolling shear which is shear in the radial-tangential plane of these lamellas, such that wood fibre roll, or slip, over each other (Salmén, 2004). This kind of shear may be critical for the load bearing capacity of floors/plates. In a previous study by Zhou et al., (2014), a three-point bending test is used to evaluate rolling shear in CLT elements. In the study the span length is presented as a factor of significance for the influence of the rolling shear (Zhou et al., 2014).

2.3.2 CLT as walls – panels subjected to in-plane bending

CLT elements are in many cases suitable for use in walls since such elements can transfer both horizontal and vertical loading. The CLT wall element dimensions are mainly limited by how manageable it is in lifting and transportation purposes during the construction phase as well as manufacturing capacities. The thickness of CLT wall elements can range between 60 mm to 300 mm, which enables manufacturing of long-height wall elements that obtains a high carrying capacity (Gustafsson, 2017).

Load bearing walls needs to carry up vertical loads from elements that are lying above and transfer the load onto the underlying construction. A wall then must be able to take up the horizontal load in the plane of the wall if the wall is determining in the stabilization of the structure. A load bearing inner wall has basically the same tasks as an load bearing outer wall. However, inner walls are also required to resist fire simultaneously from both sides (Gustafsson, 2017)

2.4 Bearing capacity in bending

A CLT element can be exposed to in-plane or out-of-plane loading depending on the load direction on the element. For walls the elements are exposed to in-plane loading while out-of-plane loading are relevant for floor elements. Three coordinate axis x-, -y - and z can be defined for a CLT element according to *Figure 4*.

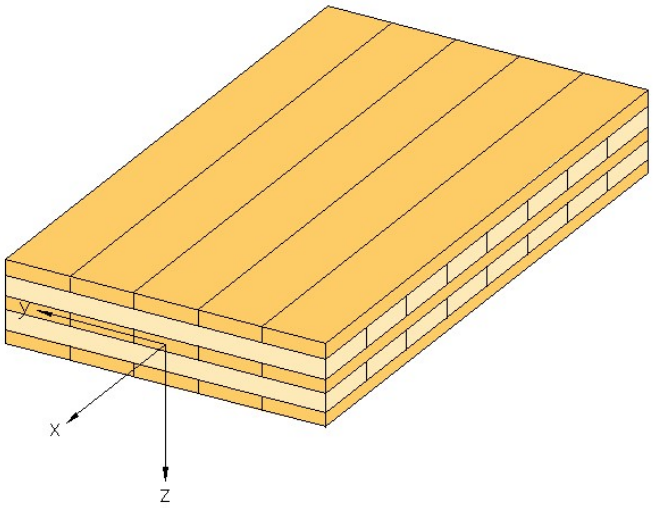

Figure 4: Illustration of the three coordinate axis x-, -, y and z for a CLT element.

For a cross-section of a CLT element variables for dimension can be defined, see *Figure 5,* and used in calculations of cross-sectional parameters. With knowledge of the dimension of the cross-section, properties such as net moment of inertia and net flexural resistance can be defined. For calculation of rough approximation on these parameters only the layers with grain orientation parallel to the load carrying direction contributes significantly and are taken into account. For a cross section perpendicular to the load carrying direction y*, see Figure 4*, the net moment of inertia is calculated as

$$I_{\mathrm{x,net}} = \frac{E_{\mathrm{x,i}}}{E_{\mathrm{ref}}}\left(\sum \frac{b_{\mathrm{x}} {t_{\mathrm{i}}}^3}{12} + \sum b_{\mathrm{x}} t_{\mathrm{i}} {a_{\mathrm{i}}}^2\right) \qquad [\mathrm{mm}^4] \qquad (2.8)$$

where $t_{\mathrm{i}} = t_1, t_3, t_5$ and $a_{\mathrm{i}} = a_1, a_3, a_5$ are the used values defined in *Figure 5*. The corresponding net flexural resistance are then calculated as

$$W_{\mathrm{x,net}} = \frac{2 \cdot I_{\mathrm{x,net}}}{h_{\mathrm{CLT}}} \qquad [\mathrm{mm}^3] \qquad (2.9)$$

(Gustafsson, 2017).

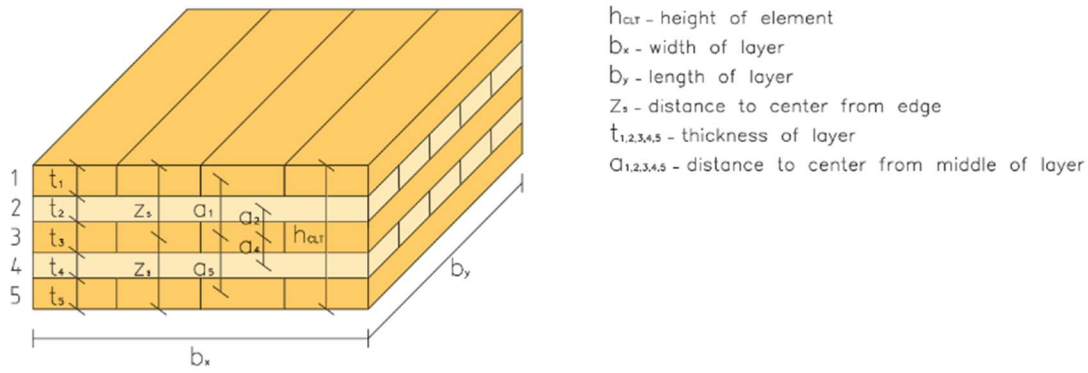

Figure 5: Definition of cross section dimensions for a CLT element.

2.4.1 Stress and stiffness

With the assumptions used in beam theory, the occurring stresses in bending for a CLT element can be illustrated according to *Figure 6* where a load perpendicular to the load carrying direction cause the stresses. As shown in *Figure 6*, it is assumed that the perpendicular layers to the load carrying direction do not contribute to the uptake of an applied load (Gustafsson, 2017). As a result of pure bending, tensile stresses occur on the side where the material is extending, i.e. the convex side of the deformed element, whilst compression stresses occurs on the concave side of the deformed element where the material is compressed. The stresses vary linearly over the cross-sectional height while being equal to zero in the cross-sectional center of gravity, also called the neutral axis. When loaded to its full potential, the maximum stress σ_{ma} occur in the element's surfaces. If the loading continues after maximum stress level has been achieved the material no longer behave linearly and failure will occur (Heyden et al., 2008).

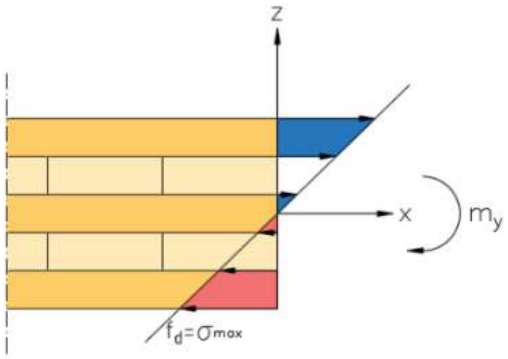

Figure 6: Tensile and compressive stress for a CLT element subjected to bending perpendicular to the plane with rotation around the y-axis.

In bending caused by moment around the supports according to *Figure 7* the bending stiffness can be calculated by knowledge of the deflection *w* in the middle of the beam, the span length *L* and the moment *m* around the supports as

$$EI_{\text{eq.1}} = \frac{L}{6w}\left(2m\left(\frac{L}{2} - \frac{\left(\frac{L}{2}\right)^3}{L^2}\right)\right) \qquad [\text{Nmm}^2] \qquad (2.10).$$

Equation *2.10*, which is denoted with the immersed letters *eq.1*, is most preferable when calculated bending stiffness from simulations since the deflection *w* can be measured from the model.
For details, see Heyden et al., (2008).

Figure 7: Elementary case for moment around supports.

Another way to retrieve values for the bending stiffness, that takes deformations caused by rolling shear into account, without knowledge of the deflection is to use the gamma method. The method originates from Eurocode 5 and implicates how to evaluate the effective moment of inertia for CLT elements of 3 or 5 layers. The theory behind the gamma method is that the middle layer is stated as a base layer, and the adjacent layers located above and below are flexibly connected to the base layer. The cross-section values are in the method depending on the span length, L_{ref}, for a simply supported beam the span is equal to the length of the beam. The span for a load is of significance and a short span increases deformation due to the impact from shear forces. For a CLT element of 5 layers with a symmetric cross-section the gamma values are the values for the parallel layers

$$\gamma_1 = \frac{1}{1+\frac{\pi^2 E_{x,1} t_1}{L_{\text{ref}}^2}\cdot\frac{t_2}{G_{\text{XY,c,2}}}} \qquad (2.11)$$

$$\gamma_3 = 1 \qquad (2.12)$$

and

$$\gamma_5 = \frac{1}{1+\frac{\pi^2 E_{x,5} t_5}{L_{\text{ref}}^2}\cdot\frac{t_5}{G_{\text{XY,c,4}}}} \qquad (2.13)$$

.

In equation (2.11), (2.12) and (2.13) $E_{x,1}$ and $E_{x,5}$ are the moduli of elasticity parallel to the fiber for layer 1 and 5, t_1 and t_5 are the distances defined in *Figure 5.* $G_{XY,c,2}$ and $G_{XY,c,4}$ are the characteristic rolling shear values for layer 2 and 4. The received gamma value from (2.11), (2.12) and (2.13) are used to evaluate the effective moment of inertia for the symmetric cross-section as:

$$I_{\text{ef}} = \frac{b_x t_1^3}{12} + \gamma_1 b_x t_1 a_1^2 + \frac{b_x t_3^3}{12} + \frac{b_x t_5^3}{12} + b_x \gamma_5 t_5 a_5^2 \tag{2.14}$$

where the constants b_x ,t_i and a_i are of the distances presented in *Figure* 55 for layer 1, 3 and 5. The bending stiffness retrieved by hand calculation, denoted with immerse letters *eq.2*, is received by

$$EI_{\text{eq.2}} = E_{1,\text{x}}\, I_{\text{ef}} \tag{2.15}$$

where $E_{\text{x},1}$ is the characteristic value for the strength class in the outer layer of the CLT element (Gustafsson, 2017). The equivalent modulus of elasticity can then be received from equation *2.10* and *2.15* as

$$E_{\text{eq.1}} = \frac{EI_{\text{eq.1}}}{I_{\text{x,net}}} \qquad \text{[MPa]} \tag{2.16}$$

and

$$E_{\text{eq.2}} = \frac{EI_{\text{eq.2}}}{I_{\text{x,net}}} \qquad \text{[MPa]} \tag{2.17}$$

2.4.2 Designed bending strength of CLT

By using the known characteristic bending strength, a design bending strength for a CLT element can be calculated as

$$f_{\text{d}} = \frac{f_{\text{k}}\, k_{\text{mod}}\, k_{\text{sys}}}{\gamma_M} \qquad \text{[MPa]} \tag{2.18}$$

where f_{k} is the characteristic bending strength of the lamellas in the outer layer, k_{mod} the strength modification factor, γ_{M} partial coefficient factor for the material and k_{sys} the factor for the system effect (Gustafsson, 2017).

By using the calculated f_{d} from (2.18) as value for maximum stress the maximal force needed to cause failure in a four-point bending test can be calculated as

$$F_{\text{max}} = 2\frac{f_{\text{d}}\, W_{\text{x,net}}}{L} \qquad \text{[N]} \tag{2.19}$$

where L is the distance from the support to the load point.

2.4.3 System effect

The final properties of a CLT element is determined by the properties of the lamellas and the previously mentioned system effect, also called lamination effect. The material properties of a single lamella have little impact on the properties of CLT elements, since the average properties of all lamellas decides element stiffness properties and have an influence on strength properties. A single lamella fails in the weakest critical cross section, which often occurs in knots, finger joints or other defected areas. In CLT elements, the risk that all weak cross sections of the lamellas coincide close to each other is small. When designing CLT element by using the characteristic values for strength (five percent fractile) of curtain strength class it is of significance to take the lamination effect into consideration. When CLT elements are exposed to loads, several lamellas collaborate causing a higher characteristic value of the element. By taking the lamination effect into consideration a higher characteristic value can be estimated. The lamination effect is represented by

$$k_{\text{sys}} = \min\begin{cases} 1.15 \\ 1 + 0.1 \cdot b \end{cases} \tag{2.20}$$

where b is the contributing width of the cross section (Gustafsson, 2017).

2.5 Standardization and assessment methods

Standards are used to specify properties of many products that we use in our everyday life. They contain technical specifications with requirements that the production companies need to fulfill. The requirements can for example concern material properties, specific items, test methods and production methods. The development of a standard is a long process where technical experts share and elaborate knowledge to establish a final standard. The aim with a standard is to provide companies with clear guidelines how to produce a product and by following a standard a company can both reduce costs and ensure a safety level in their product (Cencenelec.eu, 2019).

There are three European Standardization Organizations, CEN, CENELEC and ETSI. A document approved by one of these organizations makes the document to a European Standard (EN) valid in the European member countries. However, a standard is also voluntary, and a company have no legal obligation to apply the standard to their product. Many laws and regulations refer to standards though which makes them hard to avoid (Cencenelec.eu, 2019).

An approved and valid standard is a so-called harmonized standard (Sis.se, 2019). For CLT elements there is still no harmonized standards available. A standard that is not yet harmonized indicates that the products constructed from

that standard cannot receive CE markings. CE-markings implies that a product fulfills all the requirements in a standard and that further distribution is allowed without any additional documentation. Since CLT elements has had no harmonized standard to follow, companies make their own evaluation of the products they sell in order to receive CE markings, which they declare in an ETA (European Technical Approval). An ETA is similar to a standard with rules and instructions, though it is required to perform tests and controls in order to define the product properties. Today many companies in Europe creates their ETAs using the not yet harmonized standard prEN 16351:2018 (Gustafsson, 2017).

To establish a harmonized standard for CLT regarding testing, design, detailing and jointing is important for the future development of CLT as a construction material. One factor of great importance is to establish a standardized product definition. Such product definition could define and harmonize load bearing models. The characteristic properties of CLT could then be reliably predicted based on the characteristic properties of the raw material. This could make it easier to use raw material from local timber species with different qualities (Brandner et al., 2016).

When designing CLT elements, there is today no standard rules how to approach perforations or notches in the elements. There is neither no design approach for heterogeneous elements consisting of different timber species or quality grade. Today there is a lack of design rules and there is a need of a strength class system for the entire CLT elements. With such a system design rules regulating interaction stresses in CLT could be established (Brandner et al., 2016).

2.5.1 Standard prEN 16351:2018

The lamellas used in construction of CLT according to the standard prEN 16351:2018 needs to be strength graded according to the standard EN 14081-1. This standard state that the raw material used in CLT elements need to be strength graded boards. Common strength classes for the lamellas are C14 – C24 where the dimensions usually have a width between 80 – 200 mm and a thickness of 20 – 45 mm. The thickness of the entire CLT element cannot exceed a thickness of 500 mm. It is required according to the standard prEN 16351:2018 that each timber layer shall consist of timber from one single strength class. However, different species can be used within the same layer if strength, stiffness and density values are the same.

The measured thickness of the cross section can deviate with +/- 2 mm or 2%, whichever is greater, from the nominal thickness of the cross section, whilst the single layers can deviate with +/- 1 mm or 1%.

The adhesive used in construction needs to fulfil the requirements of the standard EN 301:2013. This standard recommends different types of adhesive that fulfils the requirements depending on the area of use. The most commonly used adhesives are phenolic and amyloplastic adhesives, along with moisture curing one-component polyurethane adhesives and emulsion polymer isocyanate adhesives.

Appliance and thickness of the adhesive could be performed by using different standards, but the recommendation from the standard EN 15416-5 states that a thickness of 0.2 mm is enough, though occurrence of exceptions does occur. For the adhesive to have a successful bonding the lamellas are allowed to have no less than 8% MC when assembling. The recommended MC in lamellas when constructing CLT elements is 12 % +/- 1 %.

However, prEN 16351:2018 consists of a variety of different generalized tests that could help determine the mechanical properties of CLT elements, there amongst shear, tensional, compressional and bending tests.

2.5.2 EN Eurocodes

Similarly, to standards, EN Eurocodes are frequently used when verifying mutual rules for dimensioning CLT elements in Europe. It consists of a series of 10 European standards, EN 1990 – EN 1999, which are meant to provide a common approach for creating building constructions in different fields of civil engineering. The purpose of EN Eurocodes are to contribute to establishing a fundamental knowledge base for construction materials and engineering in various materials. This is meant to create a more uniform level of safety for different constructions made in Europe and at the same time meet the basic requirements in constructions to bear CE Markings (Eurocodes.jrc.ec.europa.eu, 2019).

The works of EN Eurocodes can include different structural aspects of civil engineering, there amongst basic structural designs, action of structures and the design of structures in different materials such as composite steel, concrete and wood. EN Eurocodes also include geotechnical aspects, as well as structural fire design and situations including earthquake (Eurocodes.jrc.ec.europa.eu, 2019).

3. Methods

To receive the results of this investigation several methods has been used to get knowledge of the studied subject . A literature study was first performed to retrieve a foundation of knowledge about CLT. In this step much necessary information, calculation methods and theories where collected which then were used to retrieve the results of the investigation.

Regarding the adopted material properties to evaluate bending stiffness in CLT and rolling shear, several studies regarding wood properties and CLT has been analyzed. The characteristic values for clear wood properties used in this research has been determined by evaluating several studies that uses clear wood properties for Norway spruce in their evaluation. The characteristic values were retrieved from the standard EN 338:2016 which arranges relevant material properties for Norway spruce. However, this research was also evaluating bending stiffness when assuming statistically realistic values from Norway spruce originating from Sweden, Norway and Finland. The values were retrieved from a study by Olsson and Oscarsson (2017), which investigated material properties for 900 lamellas that originates from these countries that were used. This was merely done to investigate if different catchment-areas could contribute to different material properties.

3.1 Finite element simulations

Abaqus FEA 2017 (Dassault Systémes, RI, USA) is a computer aided engineering program that is used in this research. The software is specialized in finite element calculations of various materials, including orthotropic materials such as wood. The results of this research are dependent on the finite element simulations performed in this program. The different simulations are used to evaluate how quality in different layers of CLT elements effects the bending stiffness and rolling shear in the element.

When establishing a simulation model to analyze how rolling shear in lamellas are affected by different pith locations is the displacement caused by a force on a lamella measured. The displacement is recorded for 33 simulations where the pith locations changes with 5 mm each time.

To present results that shows how rolling shear in lamellas affect bending stiffness in CLT elements was a three-point bending test simulation performed in Abaqus for different span lengths of CLT elements. The results are presented as percentile comparison between different span lengths and the rolling shear modulus in the lamellas of the CLT elements.

In four-point bending test simulations two CLT constructions with changing modulus of elasticity for the lamellas is evaluated. The result of the simulations is presented as comparison between the modulus of elasticity for the entire elements to shows the significance of the raw materials mechanical properties and the perpendicular layers contribution to the overall stiffness.

3.2 Calculations according to handbook

For calculations the numerical computing software MATLAB 2018 (MathWorks, NM, USA) is used to establish calculation files with values for the desired parameters for stiffness and strength. For the four-point bending tests hand calculations are performed with equations according to Eurocode 5 from CLT-handbook (Gustafsson, 2017), also presented in *chapter 2*, to compare with the values received from the simulations.

4. Material parameters and CLT elements

The material stiffness parameters used in this investigation are according to *Table 3*. However, values of two parameters (E_L & G_{RT}) varies between simulations. This is done to achieve results showing the significance of changing these stiffness parameters. All other parameters where kept unchanged. The value for rolling shear (G_{RT}) was retrieved from Gustafsson (2017). Other parameters values are retrieved from Persson (2000).

Table 3: Material stiffness parameters for Norway spruce at a 12% moisture content used in this project.

Strength parameter	**Modulus of Elasticity [MPa]**
E_L	Modifiable value
E_R	900
E_T	650
	Shear modulus [MPa]
G_{LR}	720
G_{LT}	850
G_{RT}	Modifiable value
	Poisson's ratio
ν_{LR}/ν_R	0.018
ν_{LT}/ν_{TL}	0.013
$\nu_{RT}/\ \nu_{TR}$	0.24

4.1 Rolling shear

When investigating stiffness of a lamella to rolling shear, the modulus of elasticity in longitudinal direction, E_L, were assigned the characteristic value 11 000 MPa and the rolling shear modulus, G_{RT}, to 50 MPa. The simulations with changing pith location was then performed on a lamella of the size 120x200x20 mm.

Regarding the influence of lamella shear stiffness on stiffness of CLT elements, the value for modulus of elasticity in longitudinal direction, E_L, was set to 11 000 MPa. However, since the rolling shear stiffness (G_{RT}), is the evaluated parameter, this value is changed for each individual simulation. In the simulations four different length spans of the CLT element were simulated, with different length spans according to *Table 4.* The construction for the element was a 5-layer element with the lamella heights 40-20-40-20-40 mm and a width of the element of 700 mm for all simulations performed.

Table 4: Span length and modulus of rolling shear four the simulations.

Element	Length [mm]	Modulus of rolling shear, G_{XY} [MPa]						
1	1000	50	75	100	125	150	175	200
2	1500	50	75	100	125	150	175	200
3	2000	50	75	100	125	150	175	200
4	2500	50	75	100	125	150	175	200

4.2 Investigated combinations of layer properties

To investigate how changing strength classes in different layers affect bending stiffness in CLT elements the two CLT constructions presented in *Table 5* are simulated in four point-bending tests. In these simulations the only altered parameter value is the modulus of elasticity parallel to the fibers, E_L, though it is the parameter that has the largest influence on in-plane bending. The rolling shear modulus G_{RT} is here set to a characteristic value of 50 MPa. Values for modulus of elasticity, $E_{L,}$ is taken from the standard EN 338:2016 and from the previously mentioned study by Olsson and Oscarsson (2017). Based on results from this study mean values for dynamic MOE for boards graded into certain strength classes were used herein. The used modulus of elasticity values for the different strength classes are presented in *Table 6* and the five analyzed scenarios of strength classes in *Table 7*.

Table 5: Dimensions for the lamellas in the two analyzed constructions

	Height of the lamellas in layer 1-5 [mm]				
Construction	*1*	*2*	*3*	*4*	*5*
1	40	20	40	20	40
2	40	30	40	30	40
	Width of the lamellas in layer 1-5 [mm]				
	1	*2*	*3*	*4*	*5*
1	140	145	140	145	140
2	140	135	140	135	140

Table 6: Modulus of elasticity in longitudinal direction, E_L, for the used strength classes

	EN 338:2016			**Olsson & Oscarsson (2017)**	
Grading class	*C16*	*C24*	*C35*	*C16**	*C35**
MOE, E_L [MPa]	8000	11000	13000	10351	13253

Table 7: Strength classes for the lamellas in the studied 5 scenarios.

	Scenario				
Layer	*1*	*2*	*3*	*4*	*5*
1	C16	C24	C24	C35	C35*
2	C16	C24	C16	C16	C16*
3	C16	C24	C24	C35	C35*
4	C16	C24	C16	C16	C16*
5	C16	C24	C24	C35	C35*

5. Simulation models and calculation of bending and shear stiffness of CLT plates

5.1 Stiffness of lamellas to rolling shear

There are essentially two parameters that contributes to rolling shear, G_{xy}, in lamellas. The first is the shear modulus in the RT-plane (G_{RT}), which determines the shear moduli of the material in that direction. The second is the location of the pith, which determines the orientation of the annual rings, see *Figure 8*.

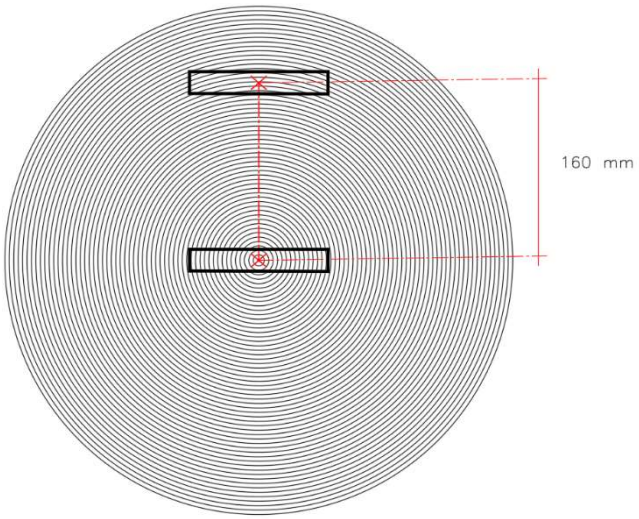

Figure 8: Start and endpoint for the 33 steps the lamella was moved in the log.

In order to analyse if rolling shear in lamellas are affected by different locations of the pith, a finite element model was created in Abaqus (2017). From this simulation an average shear strain was obtained in the lamellas XY-plane corresponding to an applied shear force (*F*), see *Figure 9*. The shear strain obtained from the FE-model were later used in equations *2.5* - *2.7* in section *2.1.4* in order to calculate shear stiffness G_{XY}.

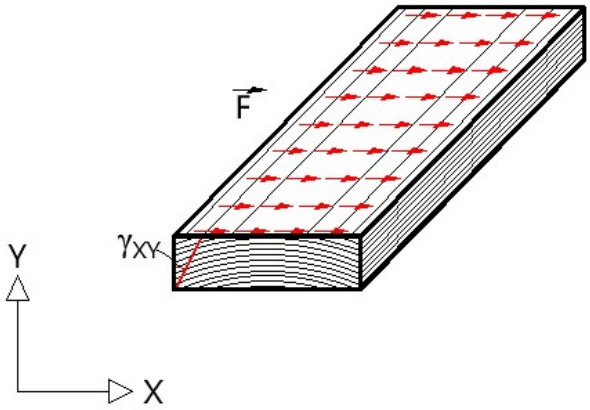

Figure 9: Illustration of the shear test preformed in Abaqus (2017) where F is the applied force and γ_{XY} the shear strain.

The simulation used to analyze the rolling shear in a lamella was a construction of two elements, see *Figure 10*. The first was a solid orthotropic element representing the lamella which was assigned material properties according to engineering constants derived with values from *Table 3*. The orthotropic element was given the dimensions 120x200x20 mm and assigned a cylindrical coordinate system, simulating the annual ring in a wood log. Since the material orientation depend on the location of the cylindrical coordinate system, the cylindrical coordinate system was adjusted 5 mm in y-direction between each simulation, see *Figure 8*, to represent the different possible locations of lamellas within the log. The second element was a solid rigid isotropic material operating as loading plate from which the horizontally located surface load, *F*, then was applied on according to *Figure 9*. However, the isotropic element was assigned a rectangular coordinate system. The orthotropic material was given a mesh of 4x3x3 mm, whilst the isotropic material was given a mesh size of 5x5x5 mm, see *Figure 10, Figure 11* and *Figure 21.* Both elements were assigned a 20-node C3D20R quadratic solid elements with reduced integration. Once the two solid elements were interactively tied together, the orthotropic element was assigned boundary condition in X-direction, Y-direction and in rotation at its base.

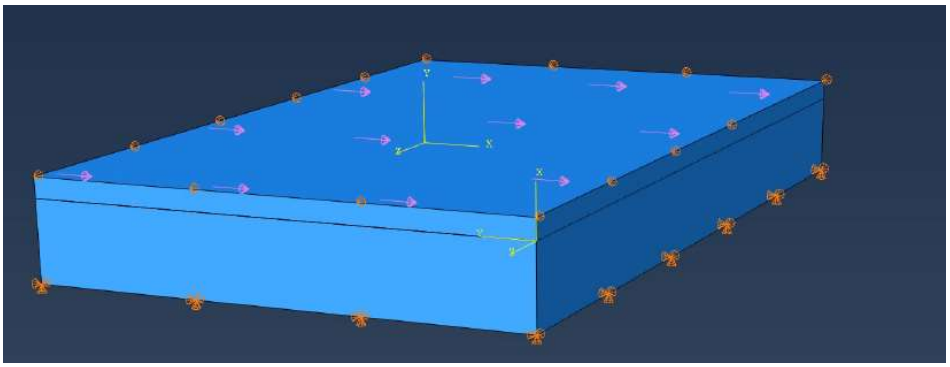

Figure 10: Shows the two elements modelled in order to simulate how pith location affects rolling shear in lamellas.

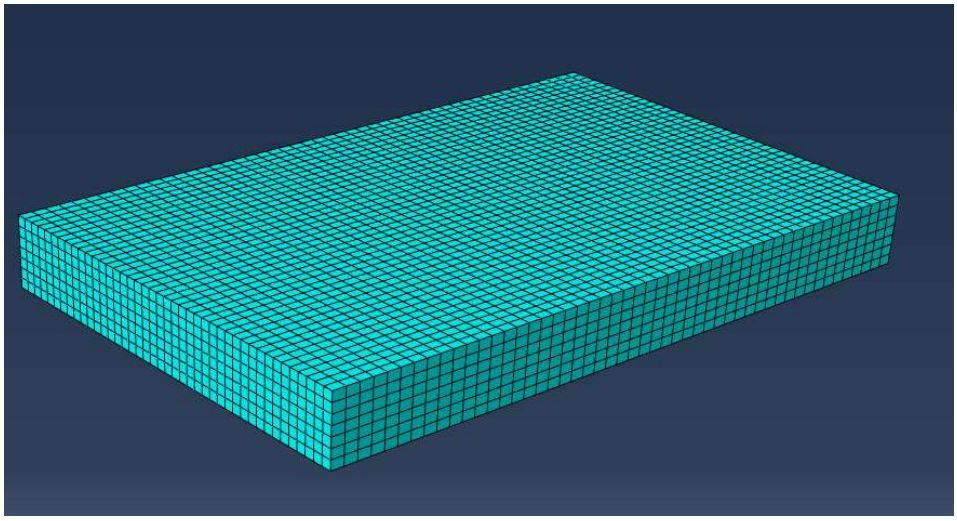

Figure 11: Shows the element mesh (element size 4x3x3mm) of the orthotropic material in analysis of rolling shear in lamellas.

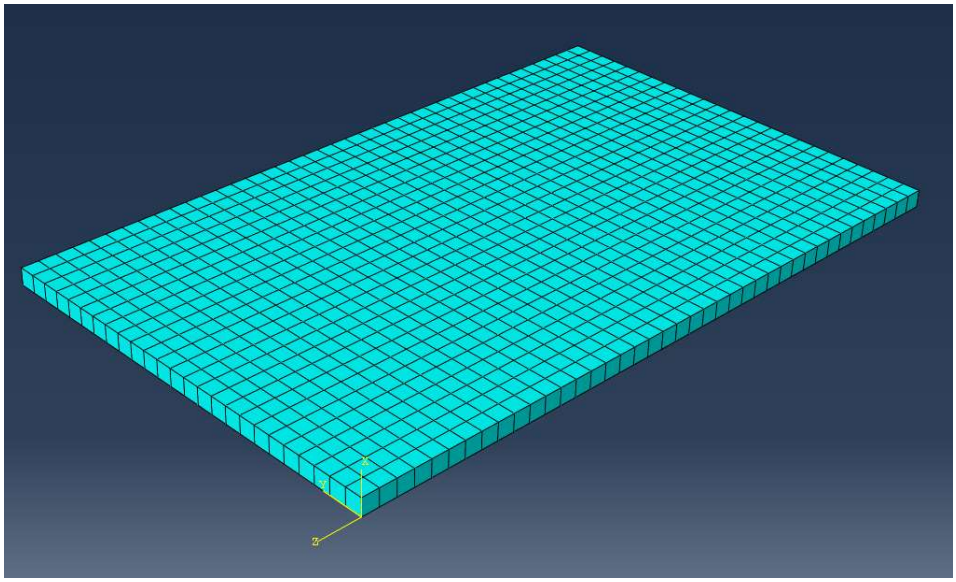

Figure 12: Element mesh (element size 5x5x5 mm) for the isotropic loading plate.

5.2 Simulation of three-point bending test and evaluation of shear deformations

To investigate the impact of rolling shear on the stiffness of CLT elements subjected to bending a three-point bending tests according to *Figure 13* was simulated in Abaqus (2017), using different span lengths, L, and values of G_{XY}. The calculated displacements at the middle of the element were recorded and compared with displacements valid for a case with negligible shear deformations.

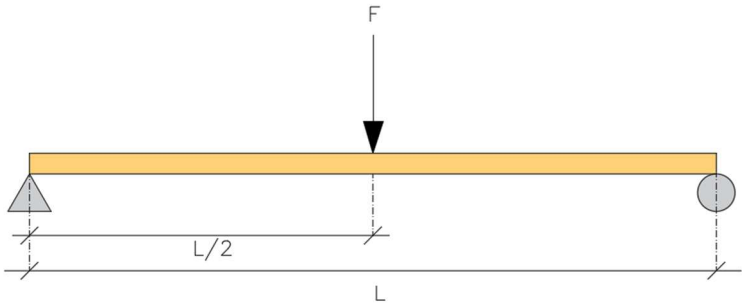

Figure 13: A three-point bending test.

For each simulation, five different layers of lamellas were modelled in Abaqus (2017). Each lamella was by use of engineering constants assigned with the decided material property and related to a Cartesian coordinate system. The assembly of the lamellas of each layer was made utilizing constraints between the edges of the adjacent lamellas and interaction ties between the layers. The assembly procedure was made this way to enable simulation of a CLT element where the lamellas has no edge glue as binder.

The assigned mesh was decided to be proportional to the lamella size, where the larger parallel layers to the base layers in layers 1, 3 and 5 were given a mesh with element sizes of 51x25x25 mm, see *Figure 14*. The perpendicularly located lamellas, layer 2 and 4, were given a mesh with element size 50x20x20 mm, see *Figure 15*. All described lamellas were assigned as 20-node C3D20R quadratic solid elements with reduced integration.

In the simulation the left rigid support on the CLT element is locked in x and y-direction, whilst the right rigid support is solely locked in y-direction. The vertically applied load in the middle of the element was 3.57 N/mm^2 (50 000 N on the entire surface) on each element and applied by using surface traction. The Abaqus model used is shown in *Figure 16.*

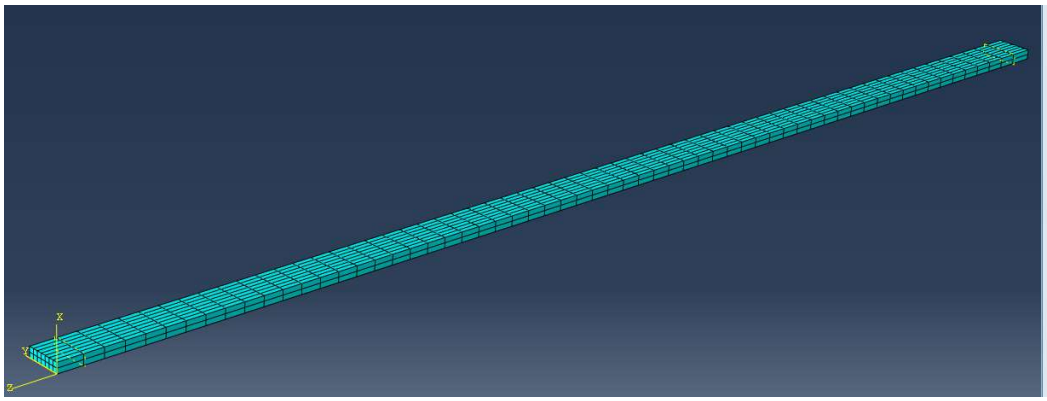

Figure 14: Description of decided element mesh size (element size 51x25x25 mm) of the first, third and fifth layers.

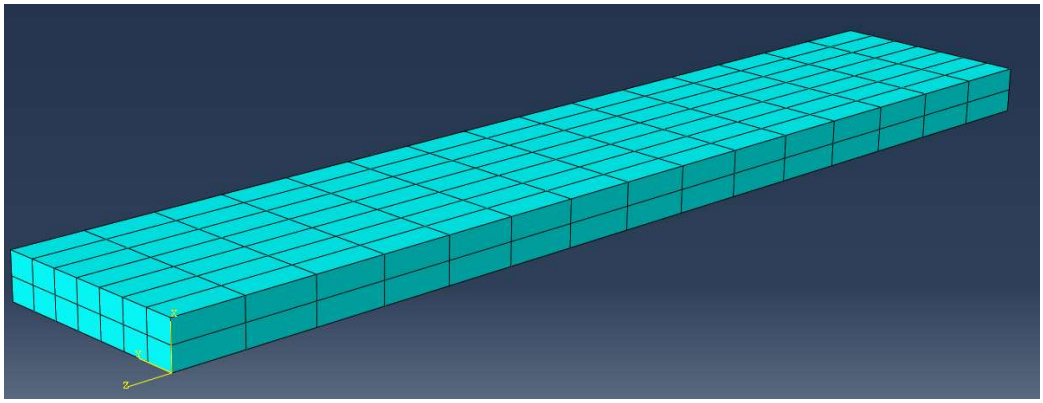

Figure 15: Description of decided element mesh size (element size 50x20x20 mm) of the second and fourth layers.

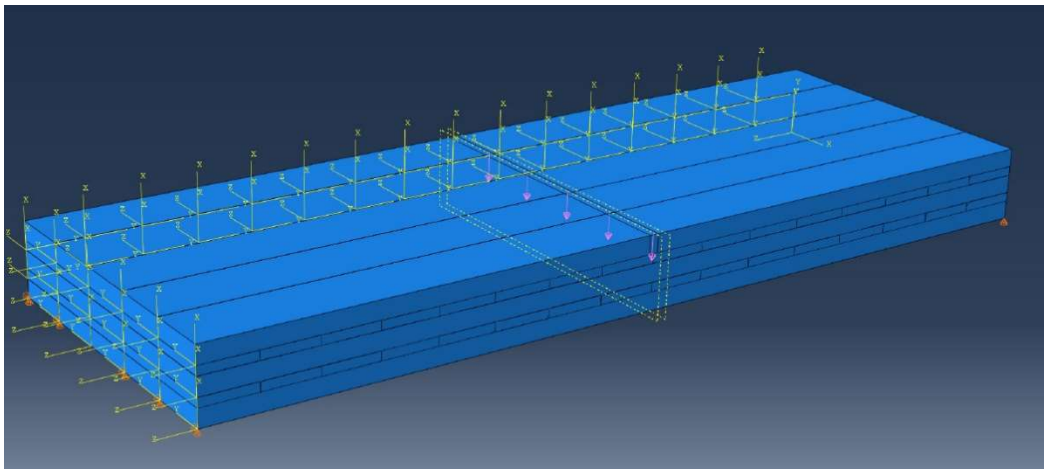

Figure 16: Three-point bending test simulation in Abaqus (2017).

5.3 Simulation of four-point bending test and evaluation of bending stiffness

To evaluate the influence of the strength classes of the laminations on the stiffness and strength of CLT elements a four-point bending test was simulated in Abaqus (2017). A four-point bending test provides no influence from shear deformation between the load points, which is preferable when solely comparing the materials strength in bending. The simulation was performed according to *Figure 17* and following the depth to span ratio for the element as specifies in the standard prEN 16531: 2018 for a four-point bending test.

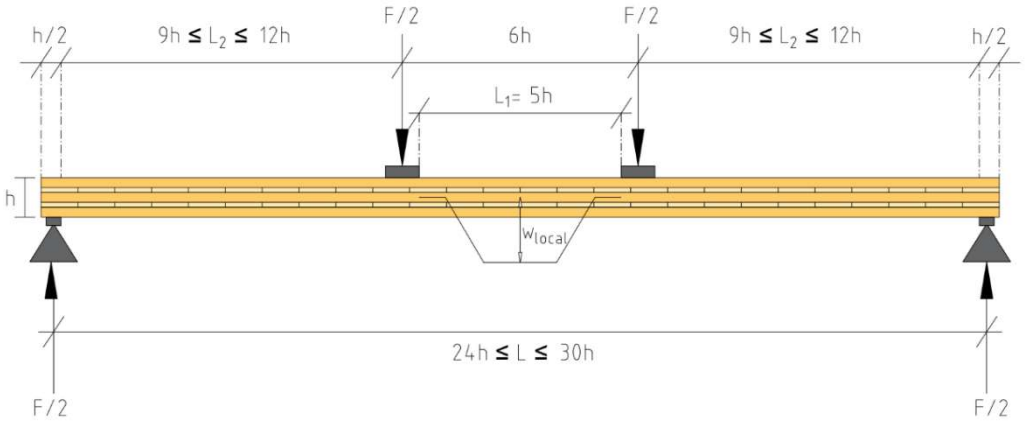

Figure 17: The proportions of a test specimen according to the standard prEN 16351:2018.

In this study, the equivalent modulus of elasticity, $E_{eq,x,}$ is evaluated from both simulations and hand calculations. When evaluating values from simulations it was necessary to obtain the effective vertical deflection, w_{local}, of the CLT element. This was done by using the relationship between w_3, w_2 and w_1, see *Figure 18.*

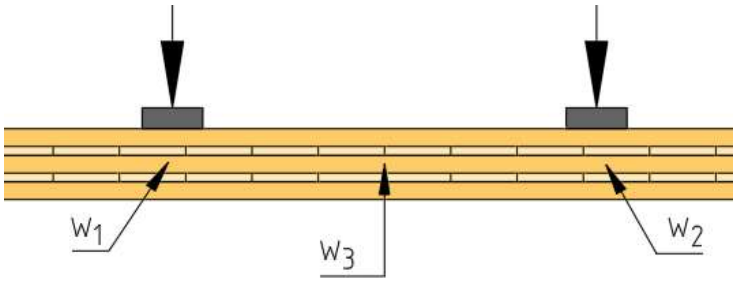

Figure 18: Location of where the deflections were measured.

The local deflection, w_{local}, was determined by evaluating the deflection that occurs beneath the loading points and the midpoint of the element. All deflection values were retrieved from the centre of the element.
The mean value of w_1 and w_2 was subtracted from w_3 in order to obtain w_{local} by

$$w_{local} = \frac{2w_3}{w_2 + w_1} \tag{5.1}$$

W_{local} was further inserted in equation *2.10* to retrieve the bending stiffness, *EI*. However, in order to evaluate the equivalent modulus of elasticity, *E*, it was necessary to calculate the net moment of inertia, $I_{x.net}$, see equation *2.8*, and insert the result in equation *2.10.*
Since it also is necessary to evaluate results by hand calculations, equations *2.11 – 2.15* were used in order to retrieve values for both the net moment of inertia and bending stiffness. These values were inserted in equation *2.17*.
This was done in order to compare values from hand calculations and simulations.
The designed bending strength and maximum load for the constructions were also evaluated with hand calculations using equations *2.18-2.20*.

The simulation models were created with the same method as the one described in section *5.2* but with changes of the parameter for the layers E_L. The total length of the CLT elements were 4800 mm, where the supports of 100 mm and location of forces were positioned to fulfill the distance requirements from the standard prEN 16351:2018. The two applied loads on the element acts on a surface of 40x725 mm each where the load is directed vertically downwards with a value of 50 000 N, defined in N/mm^2. *Figure 19* and *Figure 20* shows how the model was designed.

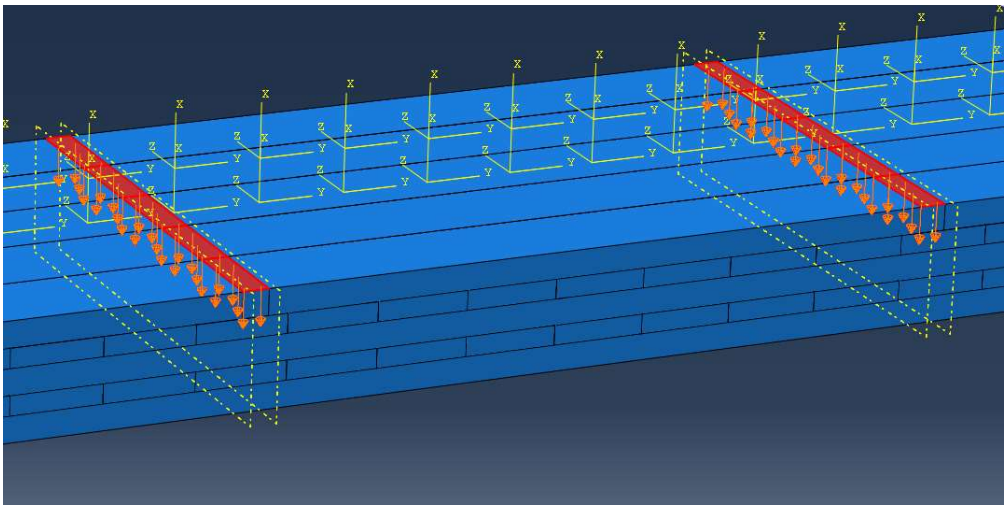

Figure 19: Shows the vertically applied surface traction acting on two surfaces á 40x735 mm areas.

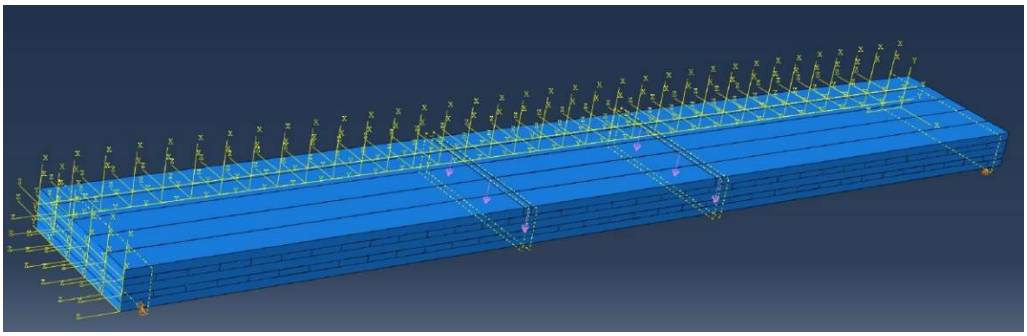

Figure 20: Four-point bending test simulation in Abaqus (2017).

6. Results and analysis

6.1 Shear stiffness of lamellas as function of pith location

The result from the Abaqus simulation described in section 5.1 for shear stiffness of a lamella is presented in *Figure 21*, where results are derived for a lamella with the dimensions 20x125 mm with calculations from *Appendix A. Figure 21* shows how the rolling shear stiffness, $G_{XY,}$ in a lamella is dependent on the distance to the pith with a decreasing value for rolling shear the further away from the pith the lamella is located. A maximum value of the average shear modulus, G_{XY}, of 161 MPa, was obtained when the pith was located at 30 mm from the center of the lamella as shown in *Figure 22.* The shear stress for the same lamella, which is about 0.5 %, is shown in *Figure 23*. In the figure the shear stress, $tau_{xy,}$ reach its maximum value when the annual rings are orientated with an angle of 45˚ from the horizonal plan. It is in these areas in the XY-plane the material can resist shear as most which results in the high values.

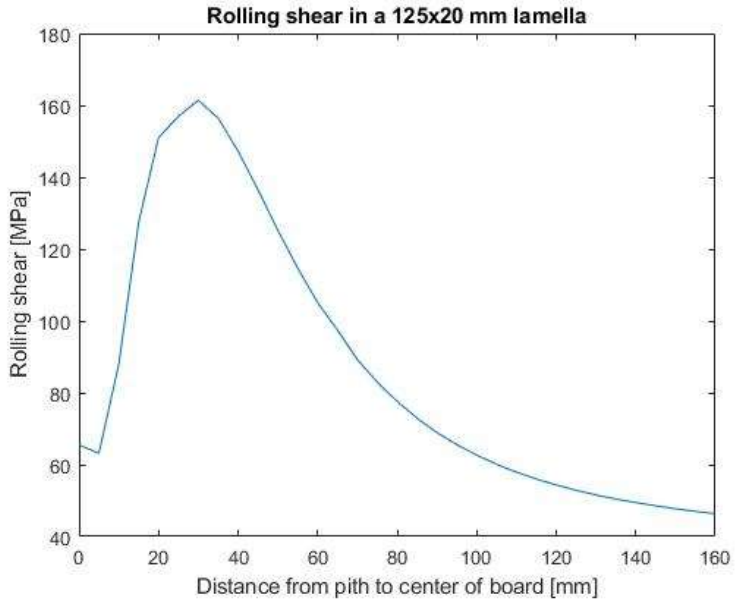

Figure 21: Modulus of rolling shear in relation to pith location.

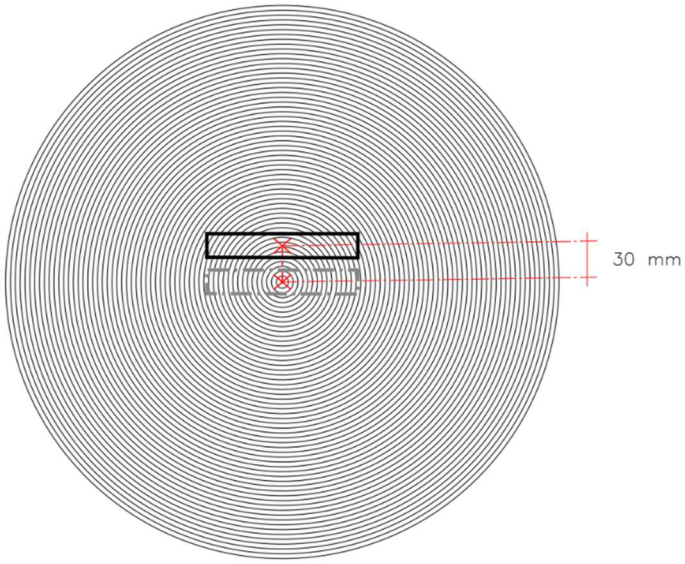

Figure 22: Location for the board with maximum value for modulus of rolling shear.

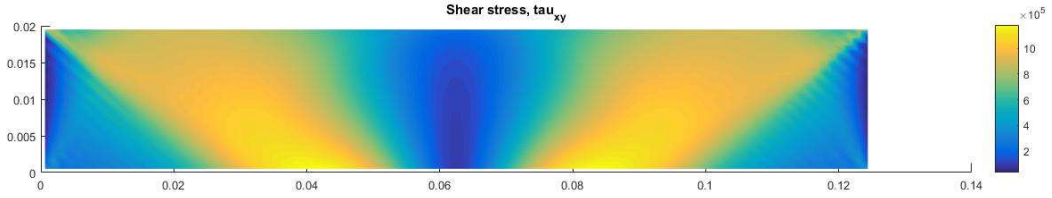

Figure 23: Distribution of rolling shear stress when the pith is located 30 mm from center of the lamella.

Before the simulation was performed, there were anticipations based on results from previous studies, see section *2.1.5*, where it is argued by authors Aicher, Christian and Hirsch (2016) that there is a correlation between stiffness to rolling shear and pith location. It was therefore anticipated that the finding in this research should correspond with the finding in the previously mentioned study. However, the mentioned study did not emphasize any crucial points from where the modulus of rolling shear was at maximum within a log. This investigation found that lamellas (center point) located 30 mm from pith had the maximum stiffness to shear in the XY-plane, and thereafter declining, for this specific geometry.

According to Gustafsson (2017) and Dinwoodie (2000) the characteristic value for modulus of rolling shear varies between 24 MPa and 50 MPa depending on collection area and measurement methods. The lower value of 24 MPa corresponds to shear in the RT-plane, not the XY-plane. However, the highest calculated value of modulus of rolling shear in this research was 161 MPa. This result indicates that there are arguments that if lamellas are located close to the pith, the characteristic value for modulus of rolling shear can be estimated to be higher, and thus more tolerant to rolling shear in the XY-plane. This result should however be further evaluated with laboratory testing.

6.2 Influence of lamella shear stiffness on CLT shear deformations

By studying the result in *Table 8* for the simulated three-point bending test it can be stated that rolling shear stiffness of lamellas has influence on the entire CLT element with a decreasing deflection for higher modulus of rolling shear. The influence of rolling shear also decreases with longer span, see *Figure 24,* where the deflections are presented in percentage depending on span length and rolling shear modulus. For a span length of 1 m the deflection is 56% higher for a rolling shear modulus of 50 MPa compared to 200 MPa. For the largest element, with span length of 2.5 m the difference in deflection is smaller, around 20%.

The results show that the modulus of rolling shear in lamellas can have considerable influence on the stiffness of the entire CLT element, decreased deflection values occurred for all the simulated span lengths as a result of an increasing modulus rolling shear. The span length showed to also have an influence, the stiffness for an element with a short span is of higher influence of a changed value of the rolling shear.

Table 8: Shows the received values from Abaqus (2017) for deflection in three-point bending.

Modulus of rolling shear, G_{XY} [MPa]	**Length of element [m]**			
	1	*1.5*	*2*	*2.5*
	Vertical Displacement [mm]			
50	1.49	3.6	5.63	9.59
75	1.27	2.69	5.11	8.90
100	1.15	2.49	4.83	8.55
125	1.07	2.37	4.67	8.33
150	1.02	2.29	4.55	8.19
175	0.99	2.23	4.47	8.08
200	0.96	2.18	4.41	8.01

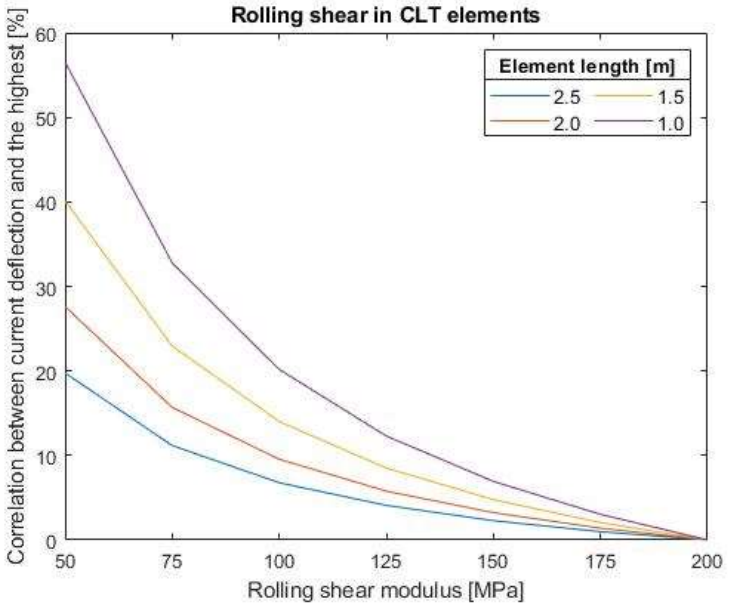

Figure 24: Deflection change in percentage from a modulus of rolling shear at 200 MPa for different span lengths when modulus of rolling shear decreases.

6.3 Influence of lamination properties on CLT bending stiffness

The results for the simulated scenarios of four-point bending test compared with hand calculation for the same test is presented by the stiffness parameter modulus of elasticity in *Table 9.* Analysis of the result indicate higher stiffness for the one that is retrieved with FEM-simulations compared with hand calculation. This may be because hand calculations are based on the gamma method which does not consider the contribution of stiffness from layers oriented perpendicular to the base layer. This is most noticeable when analyzing scenario 2 and 3 in the two constructions though.

Considering the variation in material properties between the different scenarios the result shows that usage of a mix between the strength classes C24 and C16, denoted as scenario 3, only showed little to no decrease in stiffness compared to scenario 2 were only C24 is used in all layers. The reason for the same modulus of elasticity between scenario 2 and 3 is that the material properties that differ between class C16 and C24 have negligible influence on the deformations of the lamellas oriented in perpendicular direction to the load bearing direction.

Comparison between scenarios 4 and 5 shows how difference in lamella material properties in the main direction may influence the bending stiffness in CLT elements. The statistically representative values from Olsson and Oscarsson (2017) i.e. scenario 5, shows higher stiffness in both constructions compared to the values for the strength classes from the standard EN 338:2016 used in scenario 4.

The modulus of elasticity obtained from hand calculations shows that there is difference between construction 1 and construction 2, where the thinner construction 1 shows a higher modulus of elasticity than what the thicker construction 2 does. The deviation depends on how the hand calculations are performed, especially how the gamma method evaluated the perpendicular layers. Since the total volume of perpendicular layers, which do not contribute significantly to bending stiffness, are lower in construction 1, most of the total volume consists of parallel layers that strongly contributes to bending stiffness. CLT elements constructed according to construction 1 therefore received a higher modulus of elasticity than construction 2.

Table 9: Modulus of elasticity for construction 1 and 2 for the 5 scenarios obtained by hand calculation, denoted as $E_{eq.1}$, and Abaqus simulations, denoted as $E_{eq.2}$.

Scenario	Modulus of elasticity [MPa]			
	Construction 1		*Construction 2*	
	$E_{eq.1}$	$E_{eq.2}$	$E_{eq.1}$	$E_{eq.2}$
1	5161	5221	5009	5358
2	6969	7065	6705	7229
3	6969	7065	6705	7223
4	8138	8413	7787	8417
5	8273	8610	7911	8566

Results of the four-point bending simulations shows that lamination properties influence the bending stiffness of CLT elements and that enough bending stiffness for an element can be achieved using lower quality lamellas in the perpendicular layers. According to the current standard prEN 16351:2018 it can have different qualities in each layer which carefully should be taking into account in CLT production to increase the utilization of the lamellas used in the elements. To use lower quality lamellas in the perpendicular layers could lower production costs and make better use of the available raw material.

Values obtained from hand calculation for design bending strength and maximum load for the constructions are presented in *Table 10.* To retrieve this values equation 2.18 and 2.19 has been used, where k_{sys} are calculated by equation 2.20, I_{xnet} by equation 2.8 and W_{xnet} by equation 2.9. In equation 2.18 is also γ_M=1.25 (value for Sweden) and k_{mod}=0.9 (short term action for climate class 3). The width of the cross-section *b* was set to 0.725 m and *L* defined as the length from one support to nearest load point in a four-point bending test was 1.920 m. *Appendix D* shows the calculations that was made to retrieve the values presented in *Table 10*.

It is only relevant to evaluate the parameters presented in *Table 10* for the strength classes used in the outer layers since these are exposed to the maximum stresses where failure is expected to occur. By analyzing the result is it clear that higher strength class in outer layer gives higher bending strength and that construction 2, which is thicker, can stand higher load before failure according to the calculations in this study.

Table 10: Values for designed bending strength and maximum load depending on strength class for the analyzed constructions.

C-grade of outer layer	**Designed bending strength [MPa]** f_d	**Maximum load [kN]** F_{max}	
	Construction	*Construction*	
	1 &2	*1*	*2*
C16	12.36	35.46	42.30
C24	18.53	53.19	63.45
*C35**	27.03	77.56	92.53

7. Discussion

7.1 Clear wood simulations

In all simulations the material was assumed to have clear wood properties. However, knots can have either weakening or strengthening effect in a wood product depending on analyzed property. In bending are knots often the source for failure, but for rolling shear in the RT-direction of the material knots may have a strengthening effect. For the simulation of a single lamella and its value for rolling shear modulus should probably higher values been achieved in reality because of knots in the log acting as reinforcement in the material. Further studies that investigate how knots impacts the modulus of rolling shear could therefore be of interest.

7.2 The significance of rolling shear

Previous researches have reported limited influence of rolling shear on bending stiffness in CLT elements (Aicher, Christian and Hirsch, 2016). The present investigation implies, however, that rolling shear may have a considerable impact on the deflection in the three-point bending tests, as simulated in this study. The result showed that the change of modulus of rolling shear in lamellas indeed contributed to variations in bending stiffness, especially for short elements.

Studying the result from the simulations of modulus of rolling shear in a single lamella the pith location was stated to have big influence on this strength parameter. From that result it could be interesting to evaluate how a more careful selection of lamellas, regarding modulus of rolling shear, could increase bending stiffness of CLT elements. Today there is no arrangements to perform such selections due to the current procedure in production. However, if such selections could be implemented, the utilization of raw material could contribute to a higher shear-stiffness of CLT Plates. Arguments could perhaps be made that such a procedure would increase the production cost too much in comparison with the potential benefit, and thereby make the implementation of such a procedure irrelevant.

Today the most commonly used length spans for five-layer CLT elements are ranging between 2.5 and 4 meters (Gustafsson, 2017). Since the rolling shear had lower influence the longer the CLT elements were, it can be concluded that longer spans would be even less affected. It is therefore arguable if variations in modulus of rolling shear is a very important parameter to consider since it primarily affect shorter spans, which are rarely used.

7.3 Quality of the lamellas

The perpendicular layers in a CLT element are not taken into account in many calculation methods for strength and stiffness. This is because these layers have lower contribution to the strength and stiffness compared with the parallel layers. It is therefore arguable that it is unprofitable to use lamellas with higher quality in this layer. The quality of the parallel center layer can also be discussed since this layer is not exposed to any high levels of stress.

According to beam theory, see section *2.4.14* the parallel base layer is not exposed to any high stress levels. It is therefore arguable that it is unprofitable to use lamellas with higher quality at this location. However, the considered scenarios 3-5 in this investigation were chosen to have a parallel base layer with the same quality as the outer layers. It is a possibility that use lower quality lamellas at the base layer could decrease production cost further, whilst bending stiffness may stay consistent.

The highest bending stiffness was achieved for *scenario 5*, which used a statistical approach when grading lamellas. This result indicates that higher bending stiffness can be assumed if grading of lamellas occurs due to the statistical possibility to receive higher material properties than what is required. It is therefore suggested that future studies should evaluate alternative principles for grading of lamellas to enhance the optimized construction for CLT elements.

7.4 Source of errors

To provide more reliable results from this investigation it would have been preferable to perform more tests regarding variations in material properties. This is due to diverging values from previous studies, and that geographical location of the specimens, moisture content etc. could yield different material properties in terms of modulus of elasticity, shear and Poisson´s ratio.

The modulus of elasticity in longitudinal direction was deemed to be the most relevant parameter in this research, hence it was the only considered parameter when investigating influence of lamination properties on CLT elements in bending. However, it is important to point out that other parameters could influence the result as well, even though not as significantly as E_L.

FE-analysis deals with the theoretical approach which makes fast and clear calculations according to the inserted properties in the model. However, in practice it often shows varying results since the nature of the material is more unpredictable than a simulation. To perform experimental tests in a laboratory, with result that could be compared with simulations, would contribute with valuable information regarding the validity of the results of this study.

8. Conclusions

Several results from this investigation could contribute to optimize use of material in CLT panels and to increase understanding of the significance of different material properties. The following conclusions are drawn from this study.

- CLT elements containing lamellas of lower strength classes in layers oriented perpendicular to the main load bearing direction showed little to no decrease in bending stiffness. Lower quality lamellas could therefore be used in these positions and lower the production costs.

- Pith location in lamellas affects the modulus of rolling shear, where a longer distance between pith and center of lamellas decreases the modulus of rolling shear. The highest measured modulus of rolling shear was, for a 20 × 125 mm lamella, obtained at 30 mm from the center of the lamella to the pith.

- Rolling shear affects the stiffness to bending of CLT elements. For 160 mm thick elements, and a span of 1.5 m in three-point bending, the mid-point deflection increased by approximately 56 % compared to a case where rolling shear deformations were negligible. However, the effect is much smaller for longer elements with the same thickness. For a 160 mm thick element with a span of 2.5 m the mid-point deflection was only 20 % higher, considering deformation related to rolling shear, compare to the case where rolling shear was neglected.

References

Aicher, S., Christian, Z. and Hirsch, M. (2016). *Rolling shear modulus and strength of beech wood laminations*. Holzforschung, 70(8), pp. 773-781

Aicher, S, Dill-Langer, G. (2000). *Basic Considerations to Rolling Shear Modulus in Wooden Boards*. Annual Journal on Research and Testing of Materials 11, pp. 157-165

Brander, R. and Bauer, H. (2016). *Introduction to CLT, Product Propertie*s, Strength Classes. *ReasearchGate*.

Brandner, R., Flatscher, G., Ringhofer, A., Schickhofer, G. and Thiel, A. (2016). C*ross laminated timber (CLT): overview and development. European Journal of Wood and Wood Products,* European Journal of Wood and Wood Products, 74(3), pp.331-351.

Cencenelec.eu. (2019). *What is a European Standard (EN)? - CEN-CENELEC*. [Online] Available at: https://www.cencenelec.eu/standards/DefEN/Pages/default.aspx [Accessed 11 Apr. 2019].

Dinwoodie, J. (2000). *Timber, its nature and behaviour*. London: E & FN Spon.

Dynalyse. (2019). *Precigrader - Dynalyse*. [Online] Available at: http://dynalyse.com/products/strength-grading-lumber-timber/precigrader/ [Accessed 20 May 2019].

Edholm, M. (2019). *Nya träshusfabriken ska ge 60 jobb - Dagens Arbete*. [Online] Dagens Arbete. Available at: https://da.se/2019/02/nya-trashusfabriken-ska-ge-60-jobb/ [Accessed 2019-02-20].

Eurocodes.jrc.ec.europa.eu. (2019). *Eurocodes: Building the future - The European Commission website on the Eurocodes 1*. [Online] Available at: https://eurocodes.jrc.ec.europa.eu/showpage.php?id=1 [Accessed 16 Apr. 2019].

Fellmoser, P. and Blaß, H. (2004). *Influence of rolling shear modulus on strength and stiffness of structural bonded timber elements*. [Online] Germany: University of Karlsruhe. Available at: https://pdfs.semanticscholar.org/5947/c7288b78470c120e21b4c9a28be98c2344b3.pdf [Accessed 12 May 2019].

Gustafsson, A. (2017). *KL Trähandbok*. 1st ed. Stockholm: Skogsindustrierna Svenskt Trä.

Heyden, S., Dahlblom, O., Olsson, A. and Sandberg, G. (2008). *Introduktion till strukturmekaniken*. Lund: Studentlitteratur, pp.41–43.

Karacabeyli, E. and Douglas, B. (2013). *CLT handbook*. Pointe-Claire, Québec: FPInnovations.

Lycken, A. (2006). *Appearance grading of sawn timber*. Luleå: Luleå tekniska universitet/LTU Skellefteå/Träteknologi.

Majano-Majano, A., Fernandez-Cabo, J., Hoheisel, S. and Klein, M. (2011). *A Test Method for Characterizing Clear Wood Using a Single Specimen*. Experimental Mechanics, 52(8), pp.1079-1096.

Martinsons. (2019). *Om koncernen | Martinsons*. [Online] Available at: https://www.martinsons.se/om-martinsons/koncernen/ [Accessed 11 Apr. 2019].

Matthews PC, Beech BH (1976). *Method and apparatus for detecting timber defects*. US Patent no. 3676384A

Nylinder, M. and Fryk, H. (2011). *Timmer*. Uppsala: Sveriges Lantbruksuniversitet (SLU), Institutionen för Skogens Produkter.

Olsson, A. and Oscarsson, J. (2017). Strength grading on the basis of high resolution laser scanning and dynamic excitation: a full scale investigation of performance. *European Journal of Wood and Wood Products*, 75(1), pp.17-31.

Oscarsson, J. (2014). *Strength grading of structural timber and EWP laminations of Norway spruce*. Växjö: Linnaeus University Press.

Oscarsson, J. and Blixt, J. (2016). *Förutsättning för produktion av CLT i södra Sverige - Förstudie*. Växjö: Linnéuniversitet.

Persson, K. (2000). *Micromechanical modelling of wood and fibre properties*. Lund: Lund University.

prEN 16351:2018:2015 *Träkonstruktioner - Massivträ för byggsystem – Krav*, SIS Förlag AB, 2015.

Rais, A., Ursella, E., Vicario, E. and Giudiceandrea, F. (2017). The use of the first industrial X-ray CT scanner increases the lumber recovery value: case study on visually strength-graded Douglas-fir timber. *Annals of Forest Science*, 74(2).

Salmén, L. (2004). *Micromechanical understanding of the cell-wall structure.* Comptes Rendus Biologies, 327(9-10), pp.873-880.

Sikora, K., McPolin, D. and Harte, A. (2016). *Effects of the thickness of cross-laminated timber (CLT) panels made from Irish Sitka spruce on mechanical*

performance in bending and shear. Construction and Building Materials, 116, pp.141-150.

Sis.se. (2019). *EU och Standarder*. [Online] Available at: https://www.sis.se/standarder/vad-ar-en-standard/eu-och-standarder/ [Accessed 11 Apr. 2019].

Soest J, Matthews PC, Wilson B (1993). *A simple optical scanner for grain defects. In: Proceedings of 5th international conference on scanning technology and process control for the wood products industry*, Atlanta, USA, October 25–27

SS-EN 14081-1-2016 *Träkonstruktioner - Sågat konstruktionsvirke – Del 1: Allmänna krav för visuell och maskinell hållfasthetssortering*, SIS Förlag AB, 2016.

Stapel, P. and van de Kuilen, J. (2013). *Effects of grading procedures on the scatter of characteristic values of European grown sawn timber.* Materials and Structures, 46(9), pp.1587-1598.

Säll, H. (2002). *Spiral Grain in Norway Spruce*. Växjö: Växjö University Press.

Timber Online. (2019). *CLT market keeps growing briskly*. [Online] Available at: https://www.timber-online.net/holzprodukte/2018/11/CLT-production-2017-growing-market.html [Accessed 11 Apr. 2019].
United States Patent (1993). *Method of Laminating Multiple Layers*. 5,211,792.

WoodEye AB (2019) WoodEye. http://woodeye.se/en/. [Accessed 11 May 2019]

Zhou, Q., Gong, M., Chui, Y. and Mohammad, M. (2014). *Measurement of rolling shear modulus and strength of cross laminated timber fabricated with black spruce*. Construction and Building Materials, 64, pp.379-386.

Appendices

Appendix A

```
% ------------------------------------------------------------------------------
% Rolling sher in a lamella depending on pith location obtained by displacement values
from Abaqus

% Master Theises in Structural Engineering

% 2019-05-13, Beatrice Larsson & Gustaf Lindstam

% ------------------------------------------------------------------------------
% Input values
% ------------------------------------------------------------------------------

t=20;                                          % Thickness of lamell [mm]
l=200;                                         % Length of lamell [mm]
w=125;                                         % Width of lamell [mm]
A=w*l;                                         % Sheared area [mm^2]

F=10000;                                       % Applied shear force [N]

N=[0 5 10 15 20 25 30 35 40 45 50 55 60 65 70 75 80 85 90 95 100 105 110 115 120 125 130
135 140 145 150 155 160];                      % Number of pith locations
x=[0.1222 0.1267 0.0910 0.0628 0.0530 0.0510 0.0496 0.0512 0.0544 0.0587 0.0640 0.0699
0.0763 0.0823 0.0899 0.0967 0.1034 0.1100 0.1164 0.1224 0.1281 0.1335 0.1386 0.1433
0.1477 0.1518 0.1556 0.1591 0.1623 0.1653 0.1681 0.1707 0.1731];
% Displacement in x-direction depending on pith location
y=[20.0130 20.0031 20.0021 20.0027 20.0065 20.0110 20.0158 20.0210 20.0257 20.0305
20.0350 20.0392 20.0430 20.0464 20.0493 20.0519 20.0541 20.0559 20.0573 20.0585 20.0593
20.0599 20.0602 20.0604 20.0604 20.0603 20.0600 20.0597 20.0592 20.0587 20.0581 20.0576
20.0570];     % Displacement in y-direction depending on pith location

% ------------------------------------------------------------------------------
% Output values
% ------------------------------------------------------------------------------
tao=F/A;                                       % Shear stress [N/mm2]

gamma=zeros(1,length(x));                      % Length of angle vector gamma
    for  i=1:length(x);
         gamma(i)=atan((x(i)/y(i)));           % Angle values [radian]

    end

G_r=zeros(1,length(x));                        % Length of rolling shear vector
    for n=1:length(x);
    G_r(n)=(tao/gamma(n));                     % Rolling shear values [MPa]

    end

figure
grid on
plot(N,G_r)
xlabel('Distance from pith to center of board [mm]')
```

```
ylabel('Modulus of Rolling shear [MPa]')
title('Rolling shear in a 125x20 mm lamella')
```

Appendix B

```
% ------------------------------------------------------------------------
% Deflection of a CLT element in three-point bending depending on modulus of
% rolling shear and span length

% Master Theises in structural engineering

% 2019-05-13, Beatrice Larsson & Gustaf Lindstam

% ------------------------------------------------------------------------
% Deflection values from Abaqus for the four span lengths [mm]
% ------------------------------------------------------------------------

Def_2_5=[9.5845 8.8971 8.5451 8.3306 8.1859 8.0817 8.0031]; % Span length of 2.5 m

Def_2_0=[5.6291 5.1031 4.832 4.6659 4.5534 4.4724 4.4109];  % Span length of 2.0 m

Def_1_5=[3.0592 2.6845 2.4894 2.3692 2.2875 2.2283 2.1834]; % Span length of 1.5 m

Def_1_0=[1.4964 1.2694 1.1487 1.0735 1.0221 0.9849 0.9559]; % Span length of 1.0 m

G_r=[50 75 100 125 150 175 200];                            % Modulus of rolling shear
[MPa]

%------------------------------------------------------------------------
% Creating vectors showing the deflection change in percentage compared to
% the highest modulus of rolling shear 200 MPa
%------------------------------------------------------------------------

Def_p_2_5=zeros(1,7);                                       % Vector for span length 2.5
m

     for n =1:7;
        Def_p_2_5(n)=((Def_2_5(n)/(Def_2_5(7))-1)*100);
     end

Def_p_2_0=zeros(1,7);                                       % Vector for span length 2.0
m

     for n =1:7;
        Def_p_2_0(n)=((Def_2_0(n)/(Def_2_0(7))-1)*100);
     end

Def_p_1_5=zeros(1,7);                                       % Vector for span length 1.5
m

     for n =1:7;
        Def_p_1_5(n)=((Def_1_5(n)/(Def_1_5(7))-1)*100);
     end

Def_p_1_0=zeros(1,7);                                       % Vector for span length 1.0
m

     for n =1:7;
        Def_p_1_0(n)=((Def_1_0(n)/(Def_1_0(7))-1)*100);
     end
```

```
figure                                                  % Creating graph
hold on
plot(G_r,Def_p_2_5,'DisplayName','2.5');
plot(G_r,Def_p_2_0,'DisplayName','2.0');
plot(G_r,Def_p_1_5,'DisplayName','1.5');
plot(G_r,Def_p_1_0,'DisplayName','1.0');

lgd=legend;
lgd.FontSize = 10;
lgd.Title.String = 'Element length [m]';
lgd.NumColumns=2;

xlabel('Rolling shear modulus [MPa]');
ylabel('Correlation between current deflection and the highest [%]');
title('Rolling shear in CLT elements');
```

Appendix C

```
%-------------------------------------------------------------------------
% Calculations of four-point bending around y-axis for 5-layer CLT element

% Lamellas with properties of characteristic C24 in layer 1,3,5 and C16 in  layer 2,4

% 2019-05-14 Beatrice Larsson & Gustaf Lindstam
%-------------------------------------------------------------------------
% Defintion of cross section parameters [mm]
%-------------------------------------------------------------------------

t1= 40; t2= 30; t3= 40; t4= 30; t5= 40;  % Thickness of layer 1-5 [mm]

hclt=t1+t2+t3+t4+t5;                     % Height of element [mm]

bx= 725;                                 % Width of layer [mm]
by= 4800;                                % Length of layer [mm]

Lref= by;                                % Length of span [mm]
L_9h= 9*hclt;                            % Length from support to spa[mm]
L_6h= 6*hclt;                            % Length between load points [mm]
L_w=L_6h/2;                              % Length from load point to middle of element
[mm]

a1=((hclt/2)-(t1/2));                    % Distance from center of element to center of
layer 1
a2=((hclt/2)-(t2/2));                    % Distance from center of element to center of
layer 2
a3=((hclt/2)-(t3/2));                    % Distance from center of element to center of
layer 3
a4=((hclt/2)-(t4/2));                    % Distance from center of element to center of
layer 4
a5=((hclt/2)-(t5/2));                    % Distance from center of element to center of
layer 5

%-------------------------------------------------------------------------
%Definiton of stiffness parameters for layer 1-5
%-------------------------------------------------------------------------

E_1_3_5= 11000;                          % Modulus of elasticity for layer 1,3,5
E_2_4=  8000;                            % Modulus of elasticity for layer 2,4

G9090_1_3_5= 50;                         % Rolling shear modulus in layer 1,3,5
G9090_2_4= 50;                           % Rolling shear modulus in layer 2,4

%-------------------------------------------------------------------------
% Hand calculation for 5-layer properties
%-------------------------------------------------------------------------
                                                        % Gamma values for 5-layer
CLT
gamma_1=1/(1+((pi^2*E_1_3_5*t1*t2)/(Lref^2*G9090_2_4)));     % Gamma value 1
gamma_3=1;                                              % Gamma value 3
gamma_5=1/(1+((pi^2*E_1_3_5*t5*t4)/(Lref^2*G9090_2_4)));     % Gamma value 5

I_ef= bx*(((3*t1^3)/12)+(2*gamma_1*t1*a1^2));               % Effective moment of
inertia [mm4]
```

```
I=(bx*hclt^3)/12;                                                    % Momment of inertia
according beam theory [mm4]

EI_theory=E_1_3_5*I_ef                                               % Bending stifness [Nmm^2]

E_theory=EI_theory/I                                                 % Modulus of elasticity
[MPa]

%-------------------------------------------------------------------------
% Calculation of bending stiffness with displacement values from Abaqus
%-------------------------------------------------------------------------
F=50000;                                                             % Applied load
w_1=33.35;                                                           % Displacement at load point
w_2=35.17;                                                           % Displacement in middle
w_local=w_2-w_1;                                                     % Local desplacement
M=(F/2)*(L_9h);                                                      % Moment around load point

EI_abaqus=(L_6h/(6*w_local))*(2*M*(L_w-((L_w^3)/(L_6h^2))))  % Bending stiffness [Nmm^2]

E_abaqus=EI_abaqus/I                                                 % Modulus of elasticity
[MPa]
```

Appendix D

$b_x := 725\ mm$ $b := 0.725$ $L := 1920\ mm$

$h_{CLT.1} := 160\ mm$ $h_{CLT.2} := 180\ mm$

$t_{1.1} := 40\ mm$ $t_{2.1} := 40\ mm$

$t_{1.3} := 40\ mm$ $t_{2.3} := 40\ mm$

$t_{1.5} := 40\ mm$ $t_{2.5} := 40\ mm$

$a_{1.1} := 60\ mm$ $a_{2.1} := 70\ mm$

$a_{1.3} := 0\ mm$ $a_{2.3} := 0\ mm$

$a_{1.5} := 60\ mm$ $a_{2.5} := 70\ mm$

$f_{k.16} := 16\ MPa$ $f_{k.24} := 24\ MPa$ $f_{k.35} := 35\ MPa$

$\gamma_M := 1.25$ $k_{mod} := 0.9$ $k_{sys} := 1 + (0.1\ b) = 1.073$

Designed bendning strength for C16, C24 and C35

$$f_{d.16} := \frac{f_{k.16} \cdot k_{mod} \cdot k_{sys}}{\gamma_M} = 12.355\ MPa$$

$$f_{d.24} := \frac{f_{k.24} \cdot k_{mod} \cdot k_{sys}}{\gamma_M} = 18.533\ MPa$$

$$f_{d.35} := \frac{f_{k.35} \cdot k_{mod} \cdot k_{sys}}{\gamma_M} = 27.027\ MPa$$

Values for construction 1, thickness 160 mm

$$I_{x.net.1} := \left(\frac{b_x \cdot t_{1.1}^{\,3}}{12} + \frac{b_x \cdot t_{1.3}^{\,3}}{12} + \frac{b_x \cdot t_{1.5}^{\,3}}{12} \right) + \left(b_x \cdot t_{1.1} \cdot a_{1.1}^{\,2} + b_x \cdot t_{1.3} \cdot a_{1.3}^{\,2} + b_x \cdot t_{1.5} \cdot a_{1.5}^{\,2} \right) = \left(2.204 \cdot 10^{8} \right) \ mm^4$$

$$W_{x.net.1} := \frac{2 \cdot I_{x.net.1}}{h_{CLT.1}} = \left(2.755 \cdot 10^{6} \right) \ mm^3$$

$$F_{max.1.16} := \frac{2 \cdot f_{d.16} \cdot W_{x.net.1}}{L} = 35.457 \ kN$$

$$F_{max.1.24} := \frac{2 \cdot f_{d.24} \cdot W_{x.net.1}}{L} = 53.185 \ kN$$

$$F_{max.1.35} := \frac{2 \cdot f_{d.35} \cdot W_{x.net.1}}{L} = 77.562 \ kN$$

Values for construction 2, thickness 180 mm

$$I_{x.net.2} := \left(\frac{b_x \cdot t_{2.1}^{\,3}}{12} + \frac{b_x \cdot t_{2.3}^{\,3}}{12} + \frac{b_x \cdot t_{2.5}^{\,3}}{12} \right) + \left(b_x \cdot t_{2.1} \cdot a_{2.1}^{\,2} + b_x \cdot t_{2.3} \cdot a_{2.3}^{\,2} + b_x \cdot t_{2.5} \cdot a_{2.5}^{\,2} \right) = \left(2.958 \cdot 10^{8} \right) \ mm^4$$

$$W_{x.net.2} := \frac{2 \cdot I_{x.net.2}}{h_{CLT.2}} = \left(3.287 \cdot 10^{6} \right) \ mm^3$$

$$F_{max.2.16} := \frac{2 \cdot f_{d.16} \cdot W_{x.net.2}}{L} = 42.299 \ kN$$

$$F_{max.2.24} := \frac{2 \cdot f_{d.24} \cdot W_{x.net.2}}{L} = 63.449 \ kN$$

$$F_{max.2.35} := \frac{2 \cdot f_{d.35} \cdot W_{x.net.2}}{L} = 92.53 \ kN$$

Lnu.se

Faculty of Technology
351 95 Växjö, Sweden
Telephone: +46 772-28 80 00, fax +46 470-832 17